Lawrence Livermore National Laboratory Yucca Mountain Project
Technical Highlights and Status Report
August 1994

Table of Contents

LAWRENCE LIVERMORE NATIONAL LABORATORY
(LLNL)
YUCCA MOUNTAIN SITE CHARACTERIZATION PROJECT
(YMP)
STATUS REPORT

August 1994

EXECUTIVE SUMMARY
(Items Proposed for Reporting in YMSCO or OCRWM Reports)

1) WBS 1.2.1.5, Special Studies: LLNL used thermo-hydrological models to investigate the impact of the repository depth below the ground surface (i.e., overburden thickness) on temperature-relative humidity, *T–RH*, behavior in the repository. Overburden acts like a thermal insulator or blanket, governing how long it takes for the repository heat to eventually be dissipated to the atmosphere. Removing part of this "thermal blanket" has the effect of reducing the duration of the boiling period, especially in the center of the repository. In general, removing 143.1 m of the overburden (to retain the regulatory minimum of 200 m) substantially reduces the boiling duration for thermal loads and regions with large boiling durations, modestly reduces the boiling durations for thermal loads and regions with intermediate boiling durations, and negligibly affects the boiling duration for thermal loads and regions with small boiling durations. In general, edge cooling influences the boiling duration at the repository perimeter more than the impact of overburden thickness. Also, for the shallow-overburden cases, a reduction in *RH* is associated with the end of the boiling period, relative to the reference-overburden cases. The associated reduction in temperature associated with re-wetting to more humid conditions has beneficial implications for reducing aqueous corrosion of waste packages (WPs).

2) WBS 1.2.2.3.1.1, Waste Form Testing—Spent Fuel: Unsaturated (drip) testing of spent fuel sponsored at Argonne National Laboratory by LLNL has produced uranyl oxide hydrate precipitates, a pattern consistent with the early alteration patterns observed both in unsaturated tests with UO_2 and in weathering zones of naturally occurring uraninite deposits. These uranyl oxide hydrate crystals were noted to contain Cs and K and lesser amounts of Mo and Ba. These observations suggest that the uranyl oxide hydrates may serve as a retardation process for the migration of some fission products during spent fuel corrosion.

3) WBS 1.2.2.3.1.1, Waste Form Testing—Spent Fuel: LLNL completed a series of dissolution experiments at room-temperature, with 20% oxygen, on dehydrated schoepite ($UO_3 \cdot H_2O$). Analysis of the results showed that at high carbonate concentrations (2×10^{-2} molar) the schoepite completely dissolved, probably within the first few days after the start of the room-temperature experiments. Initial dissolution rates were several hundred mgU/(m^2·day). At low carbonate concentrations (2×10^{-4} molar), for pH near both 8 and 10, dissolution rates were about 1 mgU/(m^2·day). When the experimental temperature was raised to 75°C, the dissolution rate increased and then settled back down to near 1 mgU/(m^2·day). There was ample sample remaining in the cells of the low-carbonate runs. Additional experiments were conducted with oxidized samples (U_3O_8). At high carbonate concentrations, the dissolution rates were much higher [~20 mgU/(m^2·day)] than those conducted at low carbonate concentrations [~1 mgU/(m^2·day)], but far lower than the extremely rapid schoepite release rate in high carbonate solutions. Surface areas of the U_3O_8 and the $UO_3 \cdot H_2O$ were measured at about 0.2 and 0.3 m^2/gram respectively.

4) **WBS 1.2.2.3.1.2, Waste Form Testing—Glass:** Unsaturated (drip) dissolution testing of West Valley actinide-doped glass have accumulated over seven years of data at Argonne National Laboratory, under the sponsorship of LLNL. Preliminary release rates have been determined for several of the elements of interest. These include a release rate of 2×10^{-7} g/day for boron, ~1×10^{-7} g/day for lithium, 3×10^{-9} g/day for uranium, and 7×10^{-10} g/day for neptunium.

5) **WBS 1.2.2.3.2, Metal Barriers:** Monte Carlo simulations at LLNL of potentiodynamic experiments used to determine the pitting corrosion potential have studied the separate influences of embryo birth and death on the potentiodynamic pitting potential. The model reproduces the semi-logarithmic dependence predicted by the simple birth-only model of Shibata so long as the pitting potential is not approaching zero and the induction time is not approaching the critical embryo age.

6) **WBS 1.2.2.3.2, Metal Barriers:** A Thermogravimetric Analysis Apparatus (TGA) is being developed at LLNL to measure very small changes in weight gain as a material reacts with the environment. The key parameters for such corrosion appear to be humidity, temperature, and surface condition. A new furnace arrangement was integrated into the TGA apparatus. The manufacturer supplied furnace did not give an adequate temperature control within the reaction zone for the conduct of tests. The temperature varied by 15 to 20°C within the manufacturer specified reaction zone. With the new furnace arrangement, temperature variation is 1 to 2°C within a 5-cm reaction zone. Also with the new arrangement, the reaction zone is the low temperature region within the furnace, eliminating the problem of water condensation from high humidity air on other parts of the furnace.

7) **WBS 1.2.2.3.2, Metal Barriers:** At LLNL, a scoping test was conducted on the feasibility of growing cultures for researching Microbiologically Induced Corrosion (MIC) using a quartz crystal microbalance. Soil was suspended in excess water and a sheet of copper foil was exposed. According to the literature review, microorganisms should attach to the surface and establish colonies. This was confirmed by microscopic examination which revealed bacilli and biofilm on the copper surface.

8) **1.2.2.3.3, Other Materials:** LLNL was visited by employees of SCM Metal Products, Inc., and the Copper Development Association. The visitors gave an extensive and informative presentation on boron-containing powder-metallurgy copper and copper alloys for possible use as "Basket Materials" within the waste container for the purpose of criticality-control. The information obtained will be factored into the new "Basket Materials Task" in FY95.

9) **1.2.3.4.2, Geochemical Modeling:** The independent verification & validation (V&V) Activity for EQ3/6 Version 7 was completed at LLNL. A baseline review was conducted to ascertain and document the suitability of the software for certification (qualification) for use in quality-affecting work. Only minor defects were found in Version 7.2a, the last version issued to YMP users for use in non-quality-affecting work only, pending certification. These did not adversely impact the suitability of the software for certification, and Version 7.2a was certified. The minor defects are being fixed, and corrections will be issued as part of a Version 7.2b release (this version will be "born certified"). YMP users will be notified of the certification of Version 7.2a and the plan to issue Version 7.2b.

10) **WBS 1.2.3.12.2, Hydrologic Properties of the Waste Package Environment:** At LLNL, thermo-hydrological models were used to analyze the impact of an optimized areal mass loading (AML) distribution and enhanced gas-phase diffusion on temperature and relative humidity (*T-RH*)

conditions in the repository. One of the major objectives of the optimized, nonuniform-AML distribution is to drive the entire repository environment to more uniform *T–RH* conditions. Such performance enhancement due to emplacement geometry is one way to substantiate the controlled design assumption that a given waste package design will meet the SCC requirements. A second motivation for generating more uniform, persistent reduced-*RH* conditions is to enhance performance with respect to the EBS controlled release regulatory requirement. Of the two major environmental factors affecting the rate of aqueous corrosion (*T* and *RH* on the WP surface), variations in *T* within the repository will tend to even out far earlier than variations in *RH*. During the period of substantial thermal perturbation of *RH* conditions (from ambient), *RH* conditions will never be more uniform than during the above-boiling period, while during the post-boiling period, deviations in local *RH* behavior from average behavior will tend to grow (as certain regions of the repository re-wet earlier than others), and then eventually dissipate as the entire repository has finally re-wetted to ambient (humid) conditions. Depending on what is learned from site characterization and *in situ* heater testing, the period of substantial thermal perturbation of *RH* conditions will last from several times to perhaps ten or twenty times the boiling period. Deviations will inevitably occur from the mean time to re-wet to humid conditions (with respect to aqueous corrosion) due either to proximity to the repository edge or to how heterogeneity will influence re-wetting behavior. Therefore, increasing the mean time to re-wet to humid conditions will tend to result in generally lower temperatures once relatively humid conditions have been restored, and perhaps more important for controlled release, in a greater temporal dispersion in the rate of aqueous corrosion rates from place to place within the repository. Dispersion in aqueous corrosion rates will tend to result in temporal dispersion of the distribution of WP failure times, and hence the potential source term for radionuclide transport. A dispersion in WP failure times would be more likely to meet the EBS controlled release requirement than a situation with a narrow distribution in WP failure times. This observation would be particularly true if the narrow distribution occurs at relatively early time.

11) **WBS 1.2.3.12.2, Hydrologic Properties of the Waste Package Environment:** Thermo-hydrological calculations at LLNL have been conducted to compare the Equivalent Continuum Model (ECM) with the Fracture-Matrix Model (FMM) for Repository-Heat-Driven Hydrothermal Flow. For ambient conditions, LLNL has shown in previous work that the ECM cannot represent natural infiltration generated by intense transient episodes of recharge and that it cannot be used to explain the measurement of anomalously high liquid saturations in the vitric nonwelded units such as the PTn and CHnv. In the G-Tunnel heater test, LLNL found that the ECM did very well in representing the temperature distribution and the liquid saturations in the dry-out zone; however, it could not represent the apparent condensate shedding around the boiling zone. Although no liquid saturation buildup was observed during the G-Tunnel heater test, in contrast to the ECM prediction. The magnitude of the predicted buildup can be estimated from the average condensate generated per meter of fracture during the heating stage, and a condensate flux of about 300 milliliter/day per meter of fracture is estimated. A comparison of the ECM and FMM models was conducted for an areal mass loading of 110.5 MTU/acre, using one-dimensional vertical columns through the repository horizon (thus assuming an infinite area repository). Because the comparison is for the first 80 yr, during which time edge cooling effects have not penetrated far into the repository area, this comparison is applicable to much of the repository area. Throughout the 80-yr simulation, there is outstanding agreement in both the temperature and liquid saturation profiles predicted by the two models. The agreement in predicting the relative humidity history is also outstanding. The two models predict almost identical liquid saturation profiles in the sub-boiling region (above the upper condensate zone and below the lower condensate zone) as well as in the zone of condensate buildup, including the refluxing zone above the boiling zone. In the driest part of the dry-out zone, the FMM predicts slightly larger liquid saturation than the ECM;

however, the agreement in the *RH* behavior is outstanding. The comparison was focused on early time because this is when condensate flow rates are greatest, and therefore have the greatest potential of being out of equilibrium with the matrix. For comparison with the G-tunnel heater test, the condensate flow rate in the 110.5 MTU/acre repository fracture at 80 yr is only one-twentieth of the conservative estimate for the G-Tunnel test. Additional comparisons between the ECM and the FMM are planned for larger fracture spacing and various matrix properties in order to identify conditions for which disequilibrium between fracture and matrix behavior causes the ECM to deviate from a discrete representation of fracture-matrix interaction.

12) 1.2.5.4.2, Waste Package Performance Assessment: A statistical study of the TSPA-93 data has been conducted at LLNL to understand the TSPA model's parameters and repository performance. The TSPA analysis modeled the performance of four different repository designs having two different emplacement modes and two probability distributions over the performance of each design, based on the probability distributions of 98 input parameters. The statistical analysis identified parameters that are important in predicting repository performance and studied the underlying reasons for the differences in performance of the four designs.

LLNL Deliverables Met
(August 1994)

Milestone	WBS 1.2.	Planned Date	Completion Date	Description
MOL59	3.4.2	06-01-94	08-17-94	Qualification of EQ3/6, Version 7
MOL30	3.12.2	08-31-94	08-31-94	Repository-Heat-Driven Alteration of Waste Package Environment
MOL31	3.12.2	07-29-94	08-31-94	Impact of Heterogeneity on Heat Pipes
MOL75	3.12.3	03-31-94	05-31-94	Calibrate equipment for scoping experiments
MOL91	5.4.2	03-31-94	08-08-94	ISP for the development of the YM Integrating Model (YMIM)

LLNL Deliverables Not Met
(August 1994)

Milestone	WBS 1.2.	Planned Date	Projected Date	Description	Comment
MOL01	2.3.2	07-29-94	09-30-94	Updated EBS Materials Candidate List	
MOL45	2.3.2	01-31-94	09-30-94	Submit updated Metal Barriers SIP	Delayed by TPR & NWTRB preparation
MOL94	2.3.2	07-29-94	09-30-94	Eng. Materials Characterization Report	
MOL57	2.3.5	08-01-94	09-30-94	Draft Report on Non-Metallic Barrier Materials Literature Survey	
MOL60	3.4.2	08-30-94	09-30-94	Complete V.8.0 of EQ3/6 Code Package	
MOL79	3.10.2	08-30-94	09-30-94	Rates and Magnitudes of changes in Hydrological Prop. associated with Recrystallization	
MOL04	3.10.3.1	01-12-94	09-30-94	Document core flow experiment protocol	Equip. now rebuilt and moved to new facility
MOL03	3.10.3.1	03-31-94	09-30-94	Report on colloid characterization	Delayed by equip. malfunction, related to MOL04
MOL55	3.10.3.2	08-30-94	09-30-94	Complete FY94 US Contribution to NEA -- Am Report	
MOL26	3.12.1	03-31-94	09-30-94	Topical Report on Near Field Geochemistry	Delayed by TPR & NWTRB preparation
MOL76	3.12.3	08-10-94	09-30-94	Progress Report on Simulation LBT	
MOL15	3.12.4	03-31-94	09-30-94	Large Block Excavated and Small Blocks Delivered to LLNL	Delayed by construction planning
MOL34	3.12.4	06-30-94	09-30-94	Pre-Test Calculations on Large Block Test	Will not impact LBT schedule
MOL73	3.12.5	05-31-94	09-30-94	Stability of Organic Compounds	Delayed by new ESF work
MOL89	5.4.2	06-30-94	09-30-94	YMIM Release, including User Manual	In final review

LLNL Deliverables Scheduled for the Next Reporting Period
(September 1994)

Milestone	WBS 1.2.	Planned Date	Description
MOL37	2.3.1.1	09-30-94	Interim Report. on Flow-Through Saturated Spent Fuel and UO_2 Dissolution Testing
MOL38	2.3.1.1	09-30-94	Interim Report. on Spent Fuel Oxidation TGA Testing and Modeling
MOL39	2.3.1.1	09-15-94	Interim Report on Spent Fuel Dissolution Modeling
MOL40	2.3.1.1	09-30-94	Interim Report on Oven Dry Bath Oxidation Testing and Modeling
MOL41	2.3.1.1	09-30-94	Interim Report. on Unsaturated Condition Spent Fuel Dissolution Testing
MOL43	2.3.1.2	09-30-94	Interim Report on HLW Borosilicate Glass Model Development Activities
MOL44	2.3.1.2	09-30-94	Interim Report on HLW Glass Unsaturated Testing
MOL48	2.3.2	09-30-94	Air/Steam TGA Corrosion Testing
MOL49	2.3.2	09-30-94	Corrosion Model Development
MOL50	2.3.2	09-30-94	Pitting Corrosion Testing
MOL51	2.3.2	09-30-94	Crack Propagation Testing
MOL78	3.10.1	09-30-94	Report on Code Model Capability Guidelines
MOL61	3.10.2	09-30-94	Submit Study Plan
MOL62	3.10.2	09-30-94	Report on Geochemistry aspects of Small Block Tests
MOL05	3.10.3.1	05-31-94	Cesium and Strontium Static Diffusion Test
MOL14	3.10.3.2	09-30-94	Report on Actinide Solubility Measurements at Elevated Temps. in J-13 water
MOL54	3.10.3.2	09-30-94	Report of GEMBOCHS data additions
MOL56	3.10.3.2	09-30-94	US Contributions to NEA Np/Pu Volumes and issue Rev. Contracts
MOL13	3.12.2	06-30-94	Initial Base Line V-TOUGH complete and in accordance w/ISP
MOL29	3.12.2	09-30-94	Updated code version V-TOUGH
MOL32	3.12.2	09-30-94	Study Plan (Modeling), Rev. 1
MOL80	3.12.2	09-30-94	Report. on Hydrological Prop. Meas.
MOL74	3.12.3	09-30-94	Progress Report. on Small Block Laboratory Tests at 0.5 m scale
MOL35	3.12.4	09-30-94	Prelim. Report and Data on construction experience and characterization of the small blocks and large. block.
MOL22	3.12.5	09-30-94	Prelim. Report on studies of the Degradation of Cement
MOL72	5.3.4	09-30-94	Manuscript describing the DATA0 suite of options/data
MOL87	5.4.2	09-30-94	Report Progress on EBS Trade Studies Supporting ACD
MOL90	5.4.2	09-15-94	Input to AREST II

Yucca Mountain Site Characterization Project
Variance Analysis Report
Status Thru: 31-AUG-94

PARTICIPANT: LLNL PEM: SMITH WBS: 1.2.2.3.1.1

WBS TITLE: WASTE FORM TESTING - SPENT FUEL

P&S ACCOUNT: OL2311

FY 1994 Cumulative to Date									FY 1994 at Completion					
BCWS	BCWP	ACWP	SV	SV%	SPI	CV	CV%	CPI	BAC	EAC	VAC	VAC%	IEAC	ICPI
1633	1728	1568	95	5.8	105.8	160	9.3	110.2	1785	1761	24	1.3	1620	29.5

Analysis

Cumulative Cost Variance:
The cost variance is due to two FY93 summary accounts being carried over into FY94 awaiting completion of milestones. The milestones required reports from PNL that were delayed by 30 days and as a result were not received by LLNL until mid October. These reports were immediately processed by LLNL and submitted to the Project Office for review. No actual costs were incurred but earned value was calculated upon closing of these summary accounts. These FY93 accounts were not removed during the FY93 Close-Out exercise in PACs and will continue to contribute an inaccurate $120k to both the cost and schedule variance. The correct cost variance is 40.

Cumulative Schedule Variance:
Same as above. The correct schedule variance is -25.

Variance At Complete:

Ray B Stout Sept 15, 94
P&S ACCOUNT MANAGER DATE

Dale G. Miller 9/16/94
TPO DATE

Yucca Mountain Site Characterization Project
Variance Analysis Report
Status Thru: 31-AUG-94

PARTICIPANT: LLNL PEM: SIMMONS WBS: 1.2.3.10.3.1

WBS TITLE: INTEGRATED RADIONUCLIDE RELEASE: TESTS AND MODELS

P&S ACCOUNT: OL3A31

FY 1994 Cumulative to Date									FY 1994 at Completion					
BCWS	BCWP	ACWP	SV	SV%	SPI	CV	CV%	CPI	BAC	EAC	VAC	VAC%	IEAC	TCPI
445	378	367	-67	-15.1	84.9	11	2.9	103.0	479	429	50	10.4	465	162.9

Analysis

Cumulative Cost Variance:

Cumulative Schedule Variance:

Variance At Complete:
The variance at complete is due to labor costs being less than expected because of the delay in getting qualified technical staff on board. In addition, instrument fabrication and purchase costs have been less than expected because technical progress in those areas has been hampered by understaffing, AND EQUIPMENT FAILURE.

William C. Halsey 9/16/94
P&S ACCOUNT MANAGER DATE

Lee G. Weber (for) 9/16/94
TPO DATE

Yucca Mountain Site Characterization Project
Variance Analysis Report
Status Thru: 31-AUG-94

PARTICIPANT: LLNL PEM: TYNAN WBS: 1.2.3.11.3

WBS TITLE: GEOPHYSICS-ESF SUPPORT SUBSURFACE GEOPHYSICAL TSTG

P&S ACCOUNT: 0L3E3

FY 1994 Cumulative to Date									FY 1994 at Completion					
BCWS	BCWP	ACWP	SV	SV%	SPI	CV	CV%	CPI	BAC	EAC	VAC	VAC%	TEAC	TCPI
163	163	82	0	0.0	100.0	81	49.7	198.8	180	99	81	45.0	91	100.0

Analysis

Cumulative Cost Variance:

Cumulative Schedule Variance:

Variance At Complete:
The variance at complete is due to some of the funds being used to offset a shortfall in WBS 1.2.3.5.2.2 which was only allocated $25k. The proper accounts will be charged; 1.2.3.11.3 will underrun and 1.2.3.5.2.2 will overrun; the total costs will be $205k, but with a different distribution than anticipated by YMSCO. These actions are by direction of the YMSCO Assistant Manager for Science Programs.

16 Sep 94
P&S ACCOUNT MANAGER DATE

16 Sep 94
TPO for DATE

Yucca Mountain Site Characterization Project
Variance Analysis Report
Status Thru: 31-AUG-94

PARTICIPANT: LLNL PEM: SIMMONS WBS: 1.2.3.12.1

WBS TITLE: CHEMICAL AND MINERALOGIC. PROP. OF WASTE PACKAGE

P&S ACCOUNT: 0L3C1

FY 1994 Cumulative to Date									FY 1994 at Completion					
BCWS	BCWP	ACWP	SV	SV%	SPI	CV	CV%	CPI	BAC	EAC	VAC	VAC%	IEAC	TCPI
568	599	699	31	5.5	105.5	-100	-16.7	85.7	618	713	-95	-15.4	721	135.7

Analysis

Cumulative Cost Variance:
The cumulative cost variance is due to unanticipated costs for meetings, field studies and transfer of funds.

Cumulative Schedule Variance:

Variance At Complete:
An overrun at complete will be due to unanticipated costs for Program Review meetings, unmatched expenses for field studies in which equipment had to be fabricated, rather than purchased, and the transfer of funds to accomodate external collaborations, as per Project Office changes.

Jack G. Miller 9/16/94
P&S ACCOUNT MANAGER DATE

Jack G. Miller for 9/16/94
TPO DATE

Yucca Mountain Site Characterization Project
Variance Analysis Report
Status Thru: 31-AUG-94

PARTICIPANT: LLNL PEM: SPENCE WBS: 1.2.11.1

WBS TITLE: QUALITY ASSURANCE COORDINATION AND PLANNING

P&S ACCOUNT: OLB1

FY 1994 Cumulative to Date									FY 1994 at Completion					
BCWS	BCWP	ACWP	SV	SV%	SPI	CV	CV%	CPI	BAC	EAC	VAC	VAC%	IEAC	TCPI
594	594	495	0	0.0	100.0	99	16.7	120.0	650	584	66	10.2	542	62.9

Analysis

Cumulative Cost Variance:

Cumulative Schedule Variance:

Variance At Complete:
The variance at complete is due to the inability to hire a QA Engineer as planned. Job posting was listed and no suitable internal candidates were located. Offer made externally and candidate did not accept position. A second offer has been made but not yet accepted. In addition, planned travel and training not completed due to programmatic demands.

Royce S Monfs 9-16-94
P&S ACCOUNT MANAGER DATE

Mark G. Mills 9/16/94
TPO DATE

WBS Status Sheet (WBS02) | Inc. Dollars in Thousands

WBS No. - 1.2

WBS Title - YUCCA MOUNTAIN PROJECT

Parent WBS No. -

Parent WBS Title -

Element ID - ZZ

Statement of Work

See the current WBS Dictionary

Cost/Schedule Performance

Id	Description	Current Period BCWS	BCWP	ACWP	SV	CV	FY1994 Cumulative to Date BCWS	BCWP	ACWP	SV	CV	FY1994 at Completion BAC	EAC	VAC
1.2.1	SYSTEMS ENGINEERING	13	13	14	0	-1	146	146	139	0	7	160	155	5
1.2.2	WASTE PACKAGE	300	315	479	15	-164	3167	3249	3128	82	121	3445	3422	23
1.2.3	SITE INVESTIGATIONS	642	665	845	23	-180	6179	6109	6283	-70	-174	7048	7115	-67
1.2.5	REGULATORY	134	174	155	40	19	1396	1401	1393	5	8	1545	1541	4
1.2.9	PROJECT MANAGEMENT	110	110	89	0	21	1169	1169	1172	0	-3	1282	1283	-1
1.2.11	QUALITY ASSURANCE	53	53	38	0	15	594	594	495	0	99	650	584	66
1.2.12	INFORMATION MANAGEMENT	20	20	10	0	10	229	229	214	0	15	250	237	13
1.2.13	ENVIRONMENT, SAFETY, & HEA	1	1	1	0	0	23	23	14	0	9	25	17	8
1.2.15	SUPPORT SERVICES	31	31	43	0	-12	350	350	314	0	36	382	359	23
Total		1304	1382	1674	78	-292	13253	13270	13152	17	118	14787	14713	74

Resource Distributions by Element of Cost

Fiscal Year 1994
Budgeted Cost of Work Scheduled

	Oct	Nov	Dec	Jan	Feb	Mar	Apr	May	Jun	Jul	Aug	Sep	Total
LBRHRS	8281	7278	7559	7901	7754	7732	8056	7990	7980	8062	8614	8322	95529
LABOR	762	654	658	749	710	719	730	748	727	750	767	767	8741
SUBS	109	298	264	233	315	269	218	206	226	200	142	169	2649
OTHER	155	193	147	199	175	189	217	279	265	253	387	576	3035
CAPITAL	0	0	11	21	146	59	7	81	7	0	8	22	362
Total BCWS	1026	1145	1080	1202	1346	1236	1172	1314	1225	1203	1304	1534	14787

Prepared - 09/15/94:16:56:09 | WBS Status Sheet (WBS02) | Inc. Dollars in Thousands

WBS No. - 1.2 -YUCCA MOUNTAIN PROJECT

Resource Distributions by Element of Cost

Fiscal Year 1994
Actual Cost of Work Performed

	Oct	Nov	Dec	Jan	Feb	Mar	Apr	May	Jun	Jul	Aug	Sep	Total
LBRHRS	8301	6113	5630	6247	6390	7092	7097	7530	8036	7536	8919	0	78891
LABOR	762	413	383	497	513	552	513	558	594	504	610	0	5899
SUBS	114	303	254	233	315	246	218	101	135	104	139	0	2162
OTHER	152	385	243	355	388	452	388	456	532	643	814	0	4808
CAPITAL	0	0	11	21	138	33	15	0	0	-46	111	0	283
Total ACWP	1028	1101	891	1106	1354	1283	1134	1115	1261	1205	1674	0	13152

Resource Distributions

Fiscal Year 1994	Oct	Nov	Dec	Jan	Feb	Mar	Apr	May	Jun	Jul	Aug	Sep	Total
BCWS	1026	1145	1080	1202	1346	1236	1172	1314	1225	1203	1304	1534	14787
BCWP	1188	1062	944	1048	1805	1177	1079	1048	1158	1379	1382	0	13270
ACWP	1028	1101	891	1106	1354	1283	1134	1115	1261	1205	1674	0	13152
ETC	0	0	0	0	0	0	0	0	0	0	0	1561	1561

Fiscal Year Distribution

	Prior	FY1994	FY1995	FY1996	FY1997	FY1998	FY1999	FY2000	FY2001	FY2002	FY2003	Future	At Complete
BCWS	11048	14787	32074	30997	41636	30909	20762	13287	9289	3689	823	705	210006
BCWP	10882	13270	0	0	0	0	0	0	0	0	0	0	
ACWP	10846	13152	0	0	0	0	0	0	0	0	0	0	
ETC	0	1561	32090	30976	41555	30909	20726	13398	9316	3689	823	7574	216615

MONTHLY COST/FTE REPORT

PARTICIPANT: LLNL
DATE PREPARED: 9/14/94
FISCAL MONTH/YEAR: AUG.1994

WBS ELEMENT	CURRENT MONTH END								FISCAL YEAR		
	ACTUAL COSTS	PARTICIPANT FTES	PARTICIPANT HOURS	SUBCONTRACT HOURS	PURCHASE COMMITMENTS	SUBCONTRACT COMMITMENTS	ACCRUED COSTS#	CAP EQPT ACCURAL	APPROVED BUDGET	CURRENT FY94 AFP	CUMULATIVE COSTS
1.2.1.5	14,400	0.80	128		0	0			160,000		138,600
SUBT 1.2.1	14,400	0.80	128	0	0	0	0	0	160,000	160,000	138,600
1.2.2.1	13,700	0.60	120		58	0	0		TBD		350,300
1.2.2.3.1.1	523,100	2.20	346	691	1,418	44,576	0		TBD		1,358,200
1.2.2.3.1.2	138,400	0.20	32		1,347	12,063	0		TBD		268,900
1.2.2.3.2	47,000	2.90	373		1,766	13,342	0		TBD		759,800
1.2.2.3.5	11,000	0.70	108		0	0	0		TBD		105,500
CAPITAL EQUIP.	0				1,500	0	0	0	****	91,000	133,823
SUBT 1.2.2	733,200	6.80	979	691	6,089	69,981	0	0	4,333,142	4,242,142	2,976,523
1.2.3.12.1	15,300	1.00	-50		4,382	65,773			TBD		605,500
1.2.3.12.2	85,900	3.90	661		23,430	0	19,000		TBD		742,800
1.2.3.12.3	38,500	1.70	265		35	0	19,800		TBD		217,600
1.2.3.12.4	371,900	19.50	3,134		77,723	93,102	169,795		TBD		2,149,200
1.2.3.12.5	57,800	1.70	390		297	14,760			TBD		323,800
1.2.3.10.3.1	64,300	2.00	317		20,230	0	2,500		TBD		308,100
1.2.3.10.3.2	26,000	0.80	161		680	44,996	8,900		TBD		182,100
1st SUBT 1.2.3'	659,700	30.60	4,878	0	126,777	218,631	219,995	0	TBD		4,529,100
1.2.3.1	19,100	1.00	156		0	0	0		TBD		245,400
1.2.3.4.2	39,800	1.30	210		5,250	0	0		TBD		319,500
1.2.3.5.2.2	300	0.00	0		0	0	0		TBD		64,300
1.2.3.10.1	0	0.00	0		0	0	0		TBD		90,200
1.2.3.10.2	6,400	0.50	80		0	0	0		TBD		186,500
1.2.3.11.3	20,300	0.30	60		25,965	0	0		TBD		44,400
CAPITAL EQUIP.	0	0.00	0		0	0	0		***	37,350	0
2nd SUBT 1.2.3	85,900	3.10	506	0	31,215	0	0	0	5,939,000	5,901,650	950,300
1.2.5.1	25,300	1.60	256		0	0	0		150,000		138,700
1.2.5.2.2	12,700	0.60	96		0	0	9,785		373,000		291,100
1.2.5.3.4	24,300	1.50	244		3,651	0	0		342,000		243,300
1.2.5.3.5	7,400	0.40	72		0	0	0		50,000		52,400
1.2.5.4.2	18,400	2.50	325		1,087	0	0		660,000		613,300
1.2.5.5.2	0	0.00	0		0	0	0		7,500		5,900
CAPITAL EQUIP.	0				0	0		0	**	34,000	0
SUBT 1.2.5	88,100	6.60	993	0	4,738	0	9,785	0	1,582,500	1,546,500	1,345,700

YMP PLANNING AND CONTROL SYSTEM (PACS)

MONTHLY COST/FTE REPORT

PARTICIPANT: LLNL
DATE PREPARED: 9/14/94
FISCAL MONTH/YEAR: AUG.1994

WBS ELEMENT	CURRENT MONTH END								FISCAL YEAR		
	ACTUAL COSTS	PARTICIPANT FTES	PARTICIPANT HOURS	SUBCONTRACT HOURS	PURCHASE COMMITMENTS	SUBCONTRACT COMMITMENTS	ACCRUED COSTS#	CAP EQPT ACCURAL	APPROVED BUDGET	CURRENT FY94 AFP	CUMULATIVE COSTS
1.2.9.1.2	45,900	2.10	336		1,390		0		621,000		555,900
1.2.9.2.2	42,800	3.60	578		1,655	0	1,600		662,000		613,100
SUBT 1.2.9	88,700	5.70	914	0	3,045	0	1,600	0	1,283,000	1,283,000	1,169,000
1.2.11.1	37,700	1.70	271		0	0	0		650,000		493,100
SUBT 1.2.11	37,700	1.70	271	0	0	0	0	0	650,000	650,000	493,100
										(FUNDED UNDER 1.2.16)	
1.2.12.2.2	6,800	0.30	38		0	0	0		116,000		97,800
1.2.12.2.3	3,400	0.10	18		0	0	0		134,000		115,100
SUBT 1.2.12	10,200	0.40	56	0	0	0	0		250,000	250,000	212,900
										(FUNDED UNDER 1.2.17)	
1.2.13.2.5	600	0.00	5		0	0	0		25,000		12,400
SUBT 1.2.13	600	0.00	5	0	0	0	0	0	25,000	25,000	12,400
1.2.15.2	35,000	3.20	521		99	0	0		290,000		238,700
1.2.15.3	7,300	0.30	44		0	0	0		92,000		74,000
SUBT 1.2.15	42,300	3.50	565	0	99	0	0	0	382,000	382,000	312,700
TOTAL LLNL	1,760,800	59	9,294	691	171,963	288,612	231,380	0	14,604,642	14,604,642	12,140,323

* This work was moved to WBS 1.2.3; however, funding for this work remains in Budget and Report Category DB010202 in the AFP.
**** Capital equipment budgets are included in the individual WBS Elements.
Per instructions letter dated 4/27/93 V.F. Iorii to W. L. Clarke

Issues and Concerns

None at this time.

TECHNICAL SUMMARY

1.2.1. SYSTEMS ENGINEERING

1.2.1.1 Systems Engineering Coordination and Planning

No significant activities.

1.2.1.5 Special Studies

J. Blink and T. Buscheck participated in the Thermal Loading Meeting in Las Vegas on August 24. J. Cowles of the M&O was the host. T. Buscheck gave a presentation entitled "Thermal Loading Regime Options: Pros and Cons for Above-SCP Areal Mass Loadings."

On August 22, J. Blink met with S. Saterlie and N. Jones (both of the M&O) to resolve comments on the Thermal Loading Systems Study. All comments were resolved.

J. Blink participated in the repository concept of operations exercise, with attention to performance confirmation test requirements.

J. Blink attended a FY95 Systems Studies planning meeting in Las Vegas on August 9. This meeting was helpful in preparing for the PACS upload.

Modeling Support for the Thermal Loading Systems Study

To augment the thermo-hydrological calculation support of the thermal loading systems study, LLNL has been conducting the calculations in the near-field/altered zone hydrology task with the same set of thermal loading assumptions. We assume a youngest-fuel first spent nuclear fuel (SNF) receipt scenario with a 10-yr cut-off for the youngest fuel [referred to as YFF(10)] and account for the emplacement of BWR waste packages (WPs) containing 40 assemblies per WP and PWR WPs containing 21 assemblies per WP. The waste receipt schedule was supplied by J. King of the M&O. Areal Mass Loadings (AMLs) of 24.2, 35.9, 55.3, 70, 83.4, 100, 110.5, and 150 MTU/acre have been analyzed assuming the matrix hydrological properties given in the Reference Information Base (RIB) and Klavetter and Peters (1986). We have also considered the impact of more recent matrix hydrological property data given in a recent draft report (Pruess and Tsang, 1994) that are based on measurements by Flint and others (1993). In August we focused on investigating the impact of the repository depth below the ground surface (i.e., overburden thickness) on temperature-relative humidity, *T–RH*, behavior in the repository, using the RIB and Klavetter and Peters (1986) matrix property data.

Section 1.2.3.12.2 gives a more complete picture of the calculation support for the thermal loading systems study. It discusses the sensitivity of temperature and relative humidity behavior to an optimized, nonuniform-AML distribution, with and without consideration of enhanced binary gas-phase diffusion.

Analysis of the Impact of Repository Depth on Temperature and Relative Humidity Conditions in the Repository

In past progress reports, LLNL has described the temperature T and relative humidity RH conditions throughout the repository (center to edge) for cases with a repository depth of 343.1 m

(i.e., 343.1-m-thick overburden). Table 1 summarizes the T and RH conditions for uniform-AML cases with that overburden thickness, a bulk permeability k_b = 280 millidarcy, and for "nominal" binary gas-phase diffusion, where the binary gas-phase diffusion tortuosity factor t_{eff} = 0.2. Table 3a summarizes the duration t_{bp} of the boiling period and the value of RH at the end of the boiling period for the same suite of cases. Tables 2 and 3b summarize T–RH behavior for the same suite of cases except for a 200-m-thick overburden, which was chosen because it is the shallowest overburden thickness allowed by regulation. For the reference overburden case, the repository is 225 m above the water table, while in the 200-m-thick overburden case, it is 330 m above the water table. Because of the additional 105 m standoff from the water table, the ambient liquid saturation at the repository horizon in 200-m-thick overburden case is about 10% less than in the reference-overburden case. Therefore, some of the following observations concerning RH behavior may be influenced by that factor. We plan to repeat the 200-m-thick overburden suite for the situation where the standoff to the water table is the same as in the reference-overburden case, thereby yielding a similar initial liquid saturation at the repository horizon. This case could be realistic for some of the potential expansion areas.

A comparison of Tables 3a and 3b clearly shows the role of the overburden thickness in containing the repository heat in Yucca Mountain. Effectively, the overburden acts like a thermal insulator or blanket, governing how long it takes for the repository heat to eventually be dissipated to the atmosphere. Therefore, we find that removing part of this "thermal blanket" has the effect of reducing the duration of the boiling period, t_{bp}, especially in the center of the repository. In general, removing 143.1 m of the overburden has the following effects:

1. substantially reducing t_{bp} in areas that are associated with large t_{bp}, such as
   - the entire 150-MTU/acre repository
   - the inner 90% of the 110.5-MTU/acre repository, and
   - the inner 75% of the 83.4-MTU/acre repository;
2. modestly reducing t_{bp} in areas that are associated with intermediate t_{bp}, such as
   - the inner 50% of the 55.3-MTU/acre repository,
   - the inner 75% of the 70.0-MTU/acre repository, and
   - the outer 10% of the 110.5-MTU/acre repository;
3. negligibly affecting t_{bp} in areas that are associated with small t_{bp}, such as
   - the outer 50% of the 55.3-MTU/acre repository,
   - the outer 10% of the 70.0-MTU/acre repository, and
   - the outer 3% of the 83.4-MTU/acre repository.

In general, edge cooling influences t_{bp} at the repository perimeter more than the impact of overburden thickness. We also generally observe for the shallow-overburden cases, a reduction in RH associated with the end of the boiling period relative to the reference-overburden cases.

Table 1. Repository depth = 343.1 m (reference case).
Time required to attain indicated relative humidity at various repository locations and temperature when that value of relative humidity is attained for 22.5-yr-old SNF, a gas-phase diffusion tortuosity factor $t_{eff} = 0.2$, and $k_b = 280$ millidarcy. Locations are identified as the percentage of the repository area enclosed, with 0% corresponding to the repository center and 100% corresponding to the outer perimeter.

Table 1a. AML = 55.3 MTU/acre.

	Time required to attain indicated relative humidity (yr)				Temperature when indicated relative humidity is attained (°C)			
Repository area enclosed (%)	70%	80%	90%	95%	70%	80%	90%	95%
50	670	1660	3330	4630	107	97	80	72
75	410	940	1610	2280	107	99	89	80
90	NA	200	380	490	NA	102	97	95
97	NA	NA	NA	NA	NA	NA	NA	NA

Table 1b. AML = 70 MTU/acre

	Time required to attain indicated relative humidity (yr)				Temperature when indicated relative humidity is attained (°C)			
Repository area enclosed (%)	70%	80%	90%	95%	70%	80%	90%	95%
50	3350	8700	16,150	23,560	91	69	56	49
75	1940	4080	7,630	10,450	97	77	66	61
90	630	1030	1,760	2,460	105	97	85	78
97	80	170	290	390	107	103	99	96

Table 1c. AML = 83.4 MTU/acre

	Time required to attain indicated relative humidity (yr)				Temperature when indicated relative humidity is attained (°C)			
Repository area enclosed (%)	70%	80%	90%	95%	70%	80%	90%	95%
50	8110	17,710	29,290	38,360	76	58	48	43
75	3910	8,250	13,820	19,040	86	70	59	53
90	1240	2,030	3,530	4,800	104	91	78	72
97	370	590	890	1,140	107	102	98	94

Table 1d. AML = 110.5 MTU/acre

	Time required to attain indicated relative humidity (yr)				Temperature when indicated relative humidity is attained (°C)			
Repository area enclosed (%)	70%	80%	90%	95%	70%	80%	90%	95%
50	15,960	27,910	40,990	49,980	68	54	45	42
75	9,540	15,520	24,950	32,590	76	64	53	48
90	3,190	4,890	7,460	9,890	93	82	73	68
97	1,410	1,810	2,360	2,890	106	101	93	88

Table 1e. AML = 150 MTU/acre

	Time required to attain indicated relative humidity (yr)				Temperature when indicated relative humidity is attained (°C)			
Repository area enclosed (%)	70%	80%	90%	95%	70%	80%	90%	95%
50	20,630	34,850	50,920	64,150	68	52	44	41
75	16,400	24,520	32,700	43,360	70	59	51	46
90	8,660	12,090	16,520	19,780	81	72	64	59
97	4,330	6,020	8,180	10,060	93	84	77	72

Table 2. Repository depth = 200 m.

Time required to attain indicated relative humidity at various repository locations and temperature when that value of relative humidity is attained for 22.5-yr-old SNF, a gas-phase diffusion tortuosity factor $t_{eff} = 0.2$, and $k_b = 280$ millidarcy. Locations are identified as the percentage of the repository area enclosed, with 0% corresponding to the repository center and 100% corresponding to the outer perimeter.

Table 2a. AML = 55.3 MTU/acre.

	Time required to attain indicated relative humidity (yr)				Temperature when indicated relative humidity is attained (°C)			
Repository area enclosed (%)	70%	80%	90%	95%	70%	80%	90%	95%
50	960	1820	4270	6320	105	87	61	55
75	680	1260	2640	4120	105	91	68	57
90	130	280	620	810	106	100	93	86
97	NA	NA	NA	NA	NA	NA	NA	NA

Table 2b. AML = 70 MTU/acre

	Time required to attain indicated relative humidity (yr)				Temperature when indicated relative humidity is attained (°C)			
Repository area enclosed (%)	70%	80%	90%	95%	70%	80%	90%	95%
50	4680	10,270	16,370	24,020	67	54	47	41
75	3340	7,350	12,070	18,150	69	55	48	43
90	680	1,210	2,410	3,930	104	90	68	58
97	120	200	380	560	106	102	97	93

Table 2c. AML = 83.4 MTU/acre

	Time required to attain indicated relative humidity (yr)				Temperature when indicated relative humidity is attained (°C)			
Repository area enclosed (%)	70%	80%	90%	95%	70%	80%	90%	95%
50	8300	15,510	24,760	31,050	62	50	43	39
75	6300	10,905	16,210	21,800	62	53	47	42
90	1550	3,110	5,660	8,000	91	67	57	53
97	420	680	1,090	1,500	106	101	91	82

Table 2d. AML = 110.5 MTU/acre

	Time required to attain indicated relative humidity (yr)				Temperature when indicated relative humidity is attained (°C)			
Repository area enclosed (%)	70%	80%	90%	95%	70%	80%	90%	95%
50	15,710	24,480	34,490	48,000	56	48	41	36
75	10,230	14,850	19,410	28,820	61	54	48	42
90	4,120	6,480	8,830	11,040	71	63	58	54
97	1,360	1,920	2,910	4,220	101	87	73	64

Table 2e. AML = 150 MTU/acre

	Time required to attain indicated relative humidity (yr)				Temperature when indicated relative humidity is attained (°C)			
Repository area enclosed (%)	70%	80%	90%	95%	70%	80%	90%	95%
50	30,780	45,790	68,730	100,200	48	41	35	32
75	16,930	23,230	30,370	44,000	58	51	45	40
90	8,000	10,650	13,380	17,070	68	63	58	53
97	3,600	5,190	6,870	8,680	82	72	66	62

Table 3. Uniform AML Distribution.
Duration of boiling period at various repository locations and relative humidity attained at end of boiling period for various AMLs and for 22.5-yr-old SNF, a gas-phase diffusion tortuosity factor $t_{eff} = 0.2$, and $k_b = 280$ millidarcy. Locations are identified as the percentage of the repository area enclosed, with 0% corresponding to the repository center and 100% corresponding to the outer perimeter.

Table 3a. Repository depth = 343.1 m (reference case).

Repository area enclosed (%)	Duration of boiling period (yr) and relative humidity (%) at end of boiling period for indicated AML									
	55.3 MTU/acre		70 MTU/acre		83.4 MTU/acre		110.5 MTU/acre		150 MTU/acre	
50	1760 yr	81%	2830 yr	68%	3870 yr	57%	6130 yr	44%	9590 yr	47%
75	1100 yr	84%	2000 yr	70%	2740 yr	65%	4290 yr	51%	7210 yr	45%
90	440 yr	93%	1090 yr	81%	1700 yr	77%	2870 yr	68%	5010 yr	54%
97	80 yr	98%	410 yr	96%	990 yr	92%	2150 yr	87%	3960 yr	67%

Table 3b. Repository depth = 200 m.

Repository area enclosed (%)	Duration of boiling period (yr) and relative humidity (%) at end of boiling period for indicated AMLs									
	55.3 MTU/acre		70 MTU/acre		83.4 MTU/acre		110.5 MTU/acre		150 MTU/acre	
50	1390 yr	77%	1960 yr	62%	2450 yr	55%	3600 yr	43%	5720 yr	28%
75	1070 yr	77%	1550 yr	61%	1930 yr	55%	2700 yr	48%	4170 yr	36%
90	460 yr	86%	980 yr	77%	1360 yr	68%	1960 yr	57%	2970 yr	49%
97	80 yr	97%	450 yr	92%	900 yr	86%	1590 yr	74%	2440 yr	61%

In past work we have observed that roughly 95% of the cumulative dry-out occurs during the first 1000 yr for cases where boiling effects (both convective and diffusive) dominate net moisture movement away from the dry-out zone. Because the reduction in the insulative effect of the overburden does not begin to reduce repository temperatures until after 1000 yr, it does not significantly reduce the cumulative dry-out effects. Consequently, we find in comparing Tables 1 and 2, that the duration of sub-ambient *RH* conditions at the repository is not sensitive to overburden depth. Perhaps had we adjusted the standoff to the water table to be the same (thereby, yielding nearly identical initial liquid saturation profiles), the shallow-overburden cases may have resulted in shorter periods of sub-ambient *RH* conditions than the reference-overburden cases.

As mentioned in Sec. 1.2.3.12.2 of the March progress report, all of our modeling work has assumed a value of *RH* of 98.7% in the atmosphere so that it is in vapor pressure equilibrium with the upper TCw under ambient conditions. This prevents any diffusive loss of moisture to the atmosphere under ambient conditions. As reported in March, the repository-driven temperature gradient near the ground surface is substantially greater than the temperature gradient under ambient conditions. For the reference overburden and 150-MTU/acre, the temperature gradient at the ground surface exceeds the ambient temperature gradient by a factor of 25, 8, 5, 2, and 1.1 at t = 1,000; 10,000; 20,000; 50,000; and 100,000 yr, respectively. For the shallow overburden and 150-MTU/acre, the temperature gradient at the ground surface exceeds the ambient temperature gradient by a factor of 44, 10, 6, 3, and 1.6 at the same times. The effect of a shallower overburden is to significantly steepen the temperature gradient at the ground surface relative to the reference-overburden case. In Sec. 1.2.3.12.2 of the July status report, we noted that binary gas-phase diffusion is primarily driven by temperature gradients. It is possible that binary gas-phase diffusion drives a substantial vapor flux to the atmosphere even under the ambient geothermal temperature gradient. However, because we assume *RH* = 98.7% in the atmosphere, our models do not currently yield any diffusive vapor flux to the atmosphere under ambient conditions. Had our

models represented the actual atmospheric *RH* conditions, it is likely that we would have observed:

- Moisture loss to the atmosphere under the ambient geothermal temperature gradient.
- A substantially greater repository-driven moisture loss to the atmosphere for both the reference- and shallow-overburden cases.
- The greatest atmospheric moisture loss occurs for the shallow-overburden cases, resulting in drier *RH* conditions at the repository horizon than in the reference-overburden cases.

This last observation implies that had we modeled the actual *RH* conditions in the atmosphere, repository *RH* conditions may be substantially drier for the shallow-overburden cases than for the reference-overburden cases.

Enhanced binary gas-phase diffusion would result in even larger evaporative losses to the atmosphere under both ambient and repository-disturbed conditions. It is possible that a substantial evaporative loss could significantly reduce liquid saturations all the way down to the PTn unit (and perhaps even below the PTn), thereby significantly impacting much of the condensate buildup that may occur above a high-AML repository. Shallow *in situ* heater tests are needed to better understand heat and moisture flow to the atmosphere, and to validate our models of these effects, but these tests are not in the current baseline. Adequately modeling heat and moisture flow to the atmosphere is critically important to assessing the impact of repository heat on the moisture balance in the unsaturated zone.

In addition to neglecting the diffusive moisture loss to the atmosphere, our current models have also generally assumed a zero net infiltration flux. We plan to investigate ways to explicitly incorporate evaporation and infiltration in our models, including more accurately accounting for

- *RH* of the atmosphere.
- The spatial and temporal distribution of infiltration flux.

Whatever the pre-emplacement net recharge flux distribution at Yucca Mountain is found to be, it is the net result of shallow infiltration and evaporation, driven by the ambient geothermal temperature gradient. The effective post-emplacement net recharge flux will be the net result of shallow recharge and evaporation, which may be substantially affected by repository heat for about 100,000 yr.

Because the stored repository heat in Yucca Mountain is dissipated to the atmosphere significantly earlier in the shallow-overburden cases, the temperature associated with a given value of *RH* is significantly lower than in the reference-overburden cases (compare Tables 1 and 2). For the 150-MTU/acre case, the temperature associated with *RH* = 70% is reduced by 20°C for the inner 50% of the repository and by 11 to 12°C for the outer 25% of the repository. This reduction in temperature associated with re-wetting to more humid conditions has beneficial implications for reducing aqueous corrosion of waste packages (WPs).

1.2.1.6 Configuration Management

Affected document notices were completed for CRs 94/202, 94/210M1, 94/227M1, 94/236, 94/242, 94/264, 94/270, 94/271, 94/274, 94/317, 94/318, 94/330, 94/359, and 94/369. No LLNL documents were affected.

1.2.2. WASTE PACKAGE

1.2.2.1 Waste Package Coordination and Planning

R. Stout and J. Blink gathered information on spent fuel testing needs and on ES&H consequences of testing in response to questions from the YMSCO Repository/WP Design Team Chief. A substantial part of the information was provided to YMSCO as part of a Waste Form meeting on August 30 and the Design Integration Workshop on August 31. J. Blink met with K. Izell (YMSCO) on legal issues pertaining to shipment of Approved Testing Materials from the Materials Characterization Center at PNL to Argonne National Laboratory; action was deferred until the Team Chief briefings are complete. A concise summary of testing needs for waste form characterization and metallic barrier material qualification is in preparation.

J. Blink participated in the FACD meeting in Las Vegas on August 18.

1.2.2.2 Waste Package Environment

This work is now being reported in WBS 1.2.3.12.

1.2.2.3 Waste Form and Materials Testing

1.2.2.3.1 Waste Form

1.2.2.3.1.1 Waste Form Testing—Spent Fuel

Spent Fuel Dissolution

R. Stout and S. Steward attended the International Spent Fuel Workshop in Montebello, Quebec, Canada, on August 22-24. Current LLNL uranium oxide dissolution results were presented. This meeting is the annual focus for scientists worldwide who study the characteristics of spent fuel. In addition to dissolution experiments conducted at laboratories here and abroad, oxidation, elemental speciation and mineral formation were among other spent fuel topics discussed.

D-20-43, Unsaturated Dissolution Tests with Spent Fuel

Tests under unsaturated conditions at 90°C are in progress at Argonne National Laboratory (ANL) to evaluate the long-term performance of spent fuel in the potential Yucca Mountain repository. These tests examine the leach/dissolution behavior of two types of well-characterized irradiated PWR fuels, ATM-103 and ATM-106, in three types of tests: two with a saturated water vapor atmosphere, two with a drip rate of 0.075 mL/3.5 d, and two with a higher drip rate of 0.75 mL/3.5 d. A control test without fuel but with the lower drip rate is also included. EJ-13 water for the tests came from well J-13 and was equilibrated with volcanic tuff for approximately 80 days at 90°C. The seven tests have undergone 23 months of testing at 90°C.

For the ATM-106 high-drip-rate test, the yellow-colored residue on the Zircaloy filter was examined. Alteration minerals have been noted to precipitate in relatively large amounts on test vessel components in as little as nine months of reaction (Fig. 1a). Uranyl oxide hydrates were the only precipitate identified in these early tests, a pattern consistent with the early alteration patterns observed both in unsaturated tests with UO_2 and in weathering zones of naturally occurring

uraninite deposits. These uranyl oxide hydrate crystals were noted to contain Cs and K (Fig. 1b) and lesser amounts of Mo and Ba. These observations suggest that the uranyl oxide hydrates may serve as a retardation process for the migration of some fission products during spent fuel corrosion.

Also noted in minor amounts were small spent fuel particles that had migrated from the samples and collected on the test filter plate. These particles were composed predominantly of U, with lesser Cs and Mo, and trace amounts of Ba and light-rare earth elements (Fig. 1c, Ba and rare earth elements not shown). At present, it is not known if these fuel particles were derived as fines from mechanically damaged spent fuel grains or if the particles were released during active corrosion of the intergrain boundary regions of the spent fuel fragments. For the earlier unsaturated UO_2 drip tests, intergrain boundary corrosion followed by particle spallation was found to be the dominant release mechanism during sample corrosion. Tests will continue to be monitored for the release of particles from the spent fuel tests. An increase in particulate release in future tests would suggest that the spent fuel grains are being spalled from the samples, while a decrease would be suggestive of the dissolution of particles that remained after mechanical damage of the spent fuel particles.

Video cassette recordings (VCR) of the visual appearance of each of the spent fuel tests at each test interval were edited to provide (1) separate records of each test as a function of time and (2) journal-grade photos of the visual appearance of the spent fuel as a function of time. The magnification of the macro lens used was 9.5X for most records and 20X when additional detail was desired.

Figure 1a.

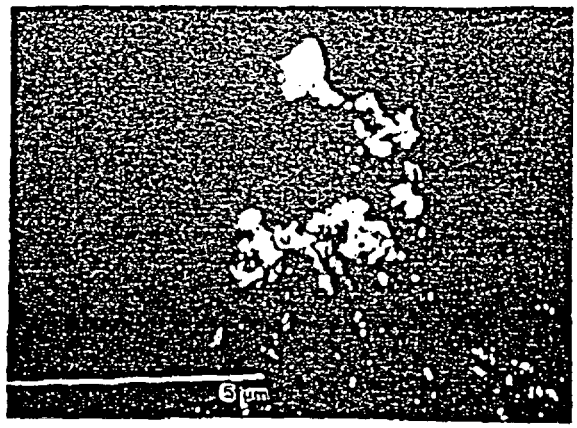

Figure 1b.

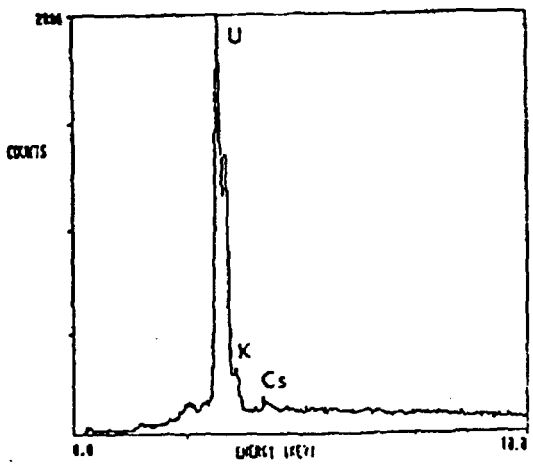

Figure 1c.

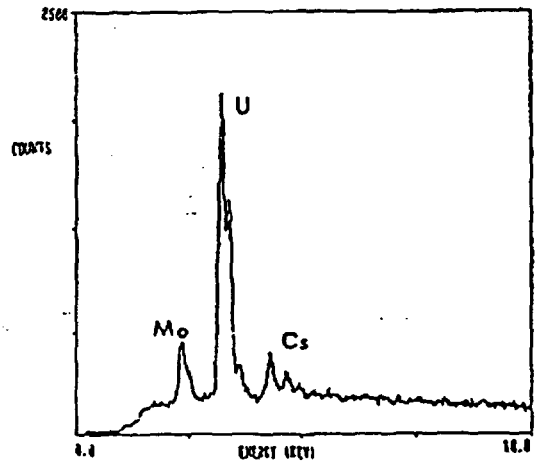

Figure 1. (a) SEM Photomicrograph of Solid Reaction Products Derived during Unsaturated Drip Tests with ATM-106 Spent Fuel after Nine Months of Reaction. The uppermost center grain is a particle of spent fuel; the remaining grains are secondary uranyl oxide hydrate crystals. (b) Scanning electron microscope/energy dispersive spectroscopy (SEM/EDS) spectrum of a uranyl oxide hydrate crystal displaying U-K-Cs composition. (c) SEM/EDS spectrum of a spent nuclear fuel particle displaying U-Mo-Cs composition.

Documentation was provided by ANL to PNL and LLNL to facilitate the shipment of spent fuel ATMs from PNL. The fuel type and sample location on specific rods was specified, per information provided by PNL. Curie content was estimated from the ORIGEN code calculations in the PNL reports for each fuel type.

Documentation for the LLNL quality assurance audit scheduled for early September was reviewed and updated.

A draft of the paper entitled "Behavior of Spent Fuel Under Unsaturated Conditions," was prepared by ANL for the American Nuclear Society sponsored meeting "DOE Spent Nuclear Fuel—Challenges and Initiatives" to be held December 13-16, 1994, and is being reviewed internally. A copy of the draft has been submitted to LLNL for programmatic review.

A draft of the annual report for the spent fuel task was prepared at ANL and is being reviewed internally.

J. Bates (ANL) attended the International Spent Fuel Workshop that was held on August 22-24, 1994, in Montebello, Quebec, and met with R. Stout (LLNL) to discuss work in progress. Two oral presentations were given:

- "Distribution of Actinides in Spent Fuel Leachate" by P. Finn (ANL) discussed the reaction of spent fuel under low water volume contact conditions anticipated to be present in the potential repository at Yucca Mountain.
- "A Comparison of the Alteration Products Formed During the Dissolution of UO_2 and Spent Nuclear Fuel Under Unsaturated Test Conditions" by D. Wronkiewicz (ANL) compares reaction products formed when UO_2 and spent fuel were reacted under the same conditions, and found a striking resemblance in the phases formed for both materials.

D-20-49.1, Unsaturated Dissolution Tests with Spent Fuel and UO_2

The objective of this Activity is to evaluate the reaction of UO_2 pellets after exposure to dripping EJ-13 water at 90°C using the Unsaturated Test Method. More specifically, these tests are designed to examine the dissolution behavior of UO_2, formation of alteration phases, release rates, and mechanisms of uranium release, and to serve as a pilot study for similar tests with spent nuclear fuel.

The results of the current nine years of experience in testing UO_2 pellets and initial observations from drip tests with spent fuel were presented at the Spent Nuclear Fuels Conference in Montebello, Quebec, in a presentation entitled "A comparison of the alteration products formed during the dissolution of UO_2 and spent nuclear fuel under unsaturated test conditions," by D. Wronkiewicz, P. Finn, J. Bates, and E. Buck.

The nonconformance YMP-001 was closed out at ANL, and the records package was transferred to LLNL. Preparations are under way at ANL for the September 8-9, 1994, audit by LLNL.

D-20-53(a), Flow-Through Dissolution Testing of UO_2

The completed room-temperature and 20% oxygen dehydrated schoepite ($UO_3 \cdot H_2O$) dissolution experiments were examined further. They showed that at high carbonate concentrations (2×10^{-2} molar) the schoepite completely dissolved, probably within the first few days after the start of the room-temperature experiments. Initial dissolution rates were several hundred mgU/(m^2·day). At

low carbonate concentrations (2×10^{-4} molar), for pH near both 8 and 10, dissolution rates were about 1 mgU/(m^2·day). When the experimental temperature was raised to 75°C, the dissolution rate increased and then settled back down to near 1 mgU/(m^2·day). There was ample sample remaining in the cells of the low-carbonate runs.

Five U_3O_8 dissolution experiments were begun early in August. As with the earlier dehydrated schoepite experiments, these were conducted at 8 ppm dissolved oxygen (20% oxygen in the gas phase) and initially at room temperature. The pH (8 to 10) and total carbonate concentration (2×10^{-4} to 2×10^{-2} molar) varied. Three of these runs are in the original test matrix. The other two are the room-temperature counterparts of 75°C matrix runs to be performed next. Similar to the earlier dehydrated schoepite runs, the dissolution rates of the U_3O_8 experiments conducted at high carbonate concentrations were much higher [~20 mgU/(m^2·day)] than those conducted at low carbonate concentrations [~1 mgU/(m^2·day)], but far lower than the extremely rapid schoepite release rate in high carbonate solutions. Surface areas of the U_3O_8 and the $UO_3 \cdot H_2O$ were measured at about 0.2 and 0.3 m^2/gram respectively.

Spent Fuel Oxidation

Activity will be discussed in a later report.

1.2.2.3.1.2 Waste Form Testing—Glass

D-20-27, Unsaturated Testing of WVDP and DWPF Glass

The N2 (Defense Waste Production Facility, DWPF, actinide-doped glass) tests continued as scheduled and have reached 103 months in length. For the N2 tests that were sampled on 6/20/94, we are continuing to analyze the samples and compile and interpret the data.

The N3 tests on West Valley actinide-doped ATM-10 glass continue as scheduled. About 85 months of testing have elapsed. The tests were last sampled in July 1994.

Preliminary release rates have been determined for several of the elements of interest. These include a release rate of 2×10^{-7} g/day for boron, ~1×10^{-7} g/day for lithium, 3×10^{-9} g/day for uranium, and 7×10^{-10} g/day for neptunium. These values do not include the amount of each element sorbed to the metal retainer component in the tests. This retainer value is expected to be greater for U and Np than for B and Li. A particular trend is that the N3#10 test consistently shows increased release of glass-related elements (Li, B, Si, U, Np, etc.) into solution relative to N3#9 and N3#12, while N3#9 displays an increased release of stainless steel-related elements (Fe, Ni) into solution. The release rate values given above are for N3#10; the values for N3#9 and #12 are about 30% lower. Boron release through 340 weeks is shown in Figure 2.

A more complete presentation of the data is being prepared for an Interim Report due in early September. The report will include analytical electron microscopy (AEM) results from colloidal material obtained from the January and July 1994 samplings.

D-20-70, Parametric Studies of WVDP and DWPF Glass

Sixteen tests continue with some in progress for up to 8 years.

Tests on a variety of glasses exposed to 60 and 95% relative humidity at 70°C continue. No test terminations have been done for several years and none are planned for this year.

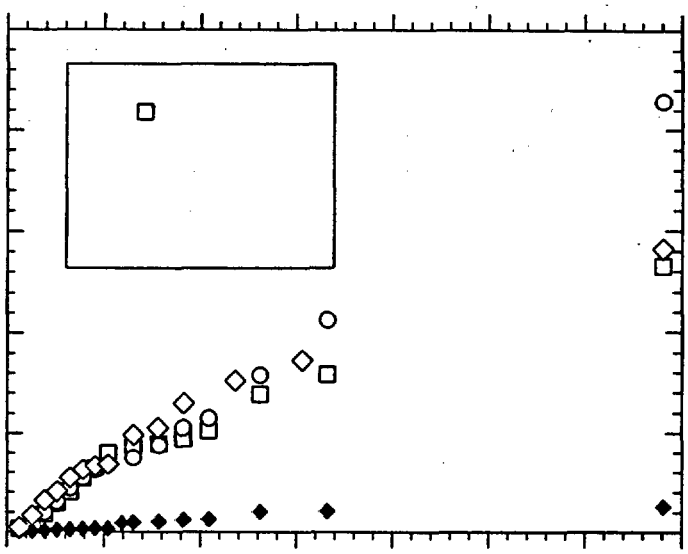

Figure 2. Cumulative Release of Boron into Solution from the N3 Tests. Note that the release for N3#10 is greater after the last sample period. This behavior was observed for several of the other measured elements. N3#11 is a blank (no glass) test. This amount of boron in N3#11 is the cumulative boron from the EJ-13 water used in the test.

1.2.2.3.2 Metal Barriers

The purpose of the metallic barrier task is to characterize the behavior and determine corrosion rates and corrosion mechanisms of metallic barriers, including the interaction with the surrounding environment. Tests, studies, and investigations are performed to determine this behavior. Conceptual models of corrosion processes are developed for use in evaluating waste package performance. This task provides considerable input on materials properties to the waste package and repository design tasks and to the performance assessment task.

Task Management and Quality Assurance (PACS OL232JCD)

Detailed planning in anticipation of a significant budget increase for FY95 continues, and estimates for acquiring test specimens and equipment in which to conduct long-term tests have been obtained.

Input was provided for budget request submissions to YMSCO. Additional planning activities for FY95 completed during August included development of a new WBS structure for the expanded "Engineered Materials" Technical Area, a 1 day planning meeting at LLNL with D. Stahl and A. Roy (M&O) on August 17, initiation of a review of several preliminary proposals from Iowa State University (D. Bullen) in the area of radiation-catalyzed aqueous corrosion, and preparation and issuance of two job postings for Principal Investigators for the expanded metallic barriers task in FY95.

Detailed planning for the out-years (FY 1996-2010) and schedule development were initiated. Royce Monks, the LLNL YMP QA Manager and G. Gdowski, visited Metal Samples, Inc. of Mumford, Alabama. They met with R. Douglas, the Quality Manager, E. Johnson, the President of the company, and D. Pritchard, the head of sales. The purpose of the visit was to evaluate the status of the company's Quality Assurance Program to determine if the YMP could use the company as a supplier. Metal Samples' Quality Assurance Program was not fully implemented at the time of the visit. Their Quality Manager does have many of the procedures written and there is a training schedule for the supervisors. They estimate full implementation of the quality program by December, 1994. They are, however, willing to push their scheduling in order to accommodate any requests that we have.

E. Dalder obtained a copy of the QA Plan for Tooling Specialists, Inc. and submitted it to LLNL-YMP QA for preliminary review. Tooling Specialists, Inc. is the supplier of Argonne National Laboratory's (ANL) test samples used in quality affecting work on our subcontract, as well as ANL's NRC supported corrosion programs. We took this step in order to develop several QA qualified fabrication sources for the large number of corrosion-test samples that will be needed for the expanded "Metallic Barriers" task in FY95.

E. Dalder, G. Gdowski, R. Van Konynenburg, D. McCright, R. Glass, M. Whitbeck, and J. Estill attended three days of training in microbiologically influenced corrosion at Structural Integrity Associates on August 29-31 in San Jose.

Prepare Planning Documents (PACS OL232LFF)

The purpose of this activity is to update the planning documents for this task, particularly the Scientific Investigation Plan (SIP) and any subsumed activity plans, to account for changes in the multipurpose container, waste package, and repository designs. The current SIP was written for the Conceptual Design phase, but the candidate materials and configuration of barriers proposed for the Advanced Conceptual Design are significantly different, necessitating an extensive revision of the SIP. Revision of the SIP is continuing, as are initiation of detailed activity plans.

Degradation Mode Surveys (PACS OL232LFA, Activity E-20-13)

The purpose of the degradation mode surveys is to amass previously published information about a candidate material and its performance in a number of environments and to interpret this body of information in the context of a potential repository in Yucca Mountain. In many cases, the degradation mode survey indicates the ways in which a material can degrade and serves to indicate the rate and kind of degradation in environments that have some similarity to what a metal barrier may experience in the Yucca Mountain setting. The lack of information in other cases suggests what work will be required to determine the behavior of the candidate material in Yucca Mountain environments.

Revision of the degradation mode survey on carbon steels and other iron-based candidate materials is continuing and completion is expected by the end of September.

Performance Tests and Model Development (PACS OL232LFB. Activity E-20-16)

The purpose of the model development activity is to derive a predictive tool that will enable using experimental data and analyses to draw long-term assessments of the performance of candidate container materials under Yucca Mountain conditions. This work will ultimately describe the performance of the multiple barrier waste package container, but as a first step in that direction, the modeling work has focused on the pitting corrosion of a corrosion resistant barrier, such as one of the nickel-base or titanium-base candidate materials. While pitting corrosion is usually governed by electrochemical, chemical, and occasionally metallurgical parameters, an important aspect of pitting is "stochastic". Much of the modeling work is aimed at developing the stochastic aspect of pitting within the electrochemical and chemical parameters. G. Henshall is the principal investigator for model development.

Details of the Modeling: Potentiodynamic Pitting Experiment Simulation

Simulations of potentiodynamic experiments used to determine the pitting potential continued in August (see the June and July reports for details of these simulations). As suggested in the July report, the focus this month was to repeat a set of simulations varying only the pit embryo death probability μ. The goal of these simulations was to separate the influences of embryo birth and death on the potentiodynamic pitting potential.

The results of these calculations are shown in Fig. 3, which shows the median pitting potential $\langle E_p \rangle$ as a function of the potential sweep velocity v for four values of μ. In these calculations, the exponential dependence of the birth probability l on the applied potential E_{app} was used:

$$l = a \exp(bE_{app}), \quad (1)$$

where a and b are constants. As in the calculations presented in Fig. 2 of the July report, $a = 2.157 \times 10^{-6}$ and $b = 321.0$ (arbitrary units).

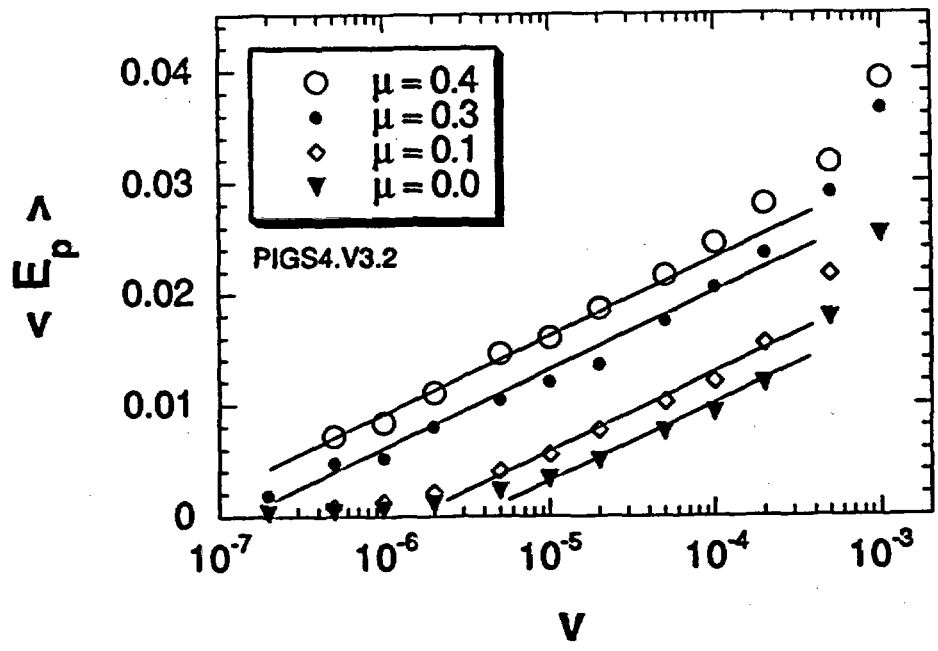

Figure 3. Pit initiation and growth stochastic (PIGS) predictions of the median pitting potential as a function of the potentiodynamic sweep velocity and the embryo death probability.

As discussed in the June and July reports, the birth-only algebraic model of Shibata and co-workers [1-3] suggests that a plot of $\langle E_p \rangle$ vs log ν should yield a straight line (on semi-log axes) when Eq. (1) is used. One might expect PIGS to reproduce these results for $\mu = 0$, since in this case there is no death of embryos, and stable pits are produced once the critical age is reached. However, Fig. 3 shows that the no-death curve is not linear on the semilogarithmic axes, except for intermediate sweep velocities. At low velocities, $\langle E_p \rangle$ approaches zero asymptotically. This behavior occurs because for $\nu = 0$ we have $E_{app} = 0$, defining a lower limit for $\langle E_p \rangle$ in the simulations. At high velocities, $\langle E_p \rangle$ increases rapidly with increasing ν. This nonlinearity (on semilogarithmic axes) appears to be related to the fact that at high ν, and therefore large E_{app}, the median number of time steps required to form a stable pit approaches the critical embryo age input into the model (10 steps for the simulations reported in Fig. 3).

As μ is increased, Fig. 3 shows that the pitting potential increases for a given sweep velocity. This is expected since embryo death will generally increase the number of time steps, and thus the potential for a given sweep velocity, required to form a stable pit. Within the linear regime for each curve, the slopes are essentially independent of μ. Increasing μ only has the effect of increasing the range of velocities over which the linear regime is exhibited. The cause for this expansion of the linear range at low ν appears to be that $\langle E_p \rangle$ increases with increasing μ, thus reducing the value of ν for which the nonlinear, asymptotic decrease in $\langle E_p \rangle$ toward zero occurs. At high velocities, the nonlinear increase in $\langle E_p \rangle$ with increasing log ν appears to occur at essentially the same value of ν for all values of μ. This behavior is consistent with the observation

that this non linearity occurs when the median number of time steps required to form a stable pit approaches the critical embryo age.

In conclusion, it appears that the PIGS model reproduces the linear dependence between $<E_p>$ and log ν predicted by the simple birth-only model of Shibata so long as the pitting potential is not approaching zero and the induction time is not approaching the critical embryo age.

References

1. T. Shibata and T. Takeyama, *Corr.* 33 (1977) 243.
2. T. Shibata, *Corr. Sci.* 31 (1990) 413.
3. T. Shibata and T. Takeyama, in *Proc. Second Japan-U.S.S.R. Corrosion Seminar, JSCE* (1980) p. 178.

Parameter Tests and Metal Degradation (PACS OL232LFC, Activity E-20-17)

There are currently two active parametric studies, one on thermogravimetric analysis and the other on corrosion sensor development, including support to the Large Block Test.

Thermogravimetric Analysis

The purpose of this work is determination of the conditions under which aqueous corrosion processes occur after emplacement of the waste package. These conditions have special significance in an unsaturated zone repository, because the extent of degradation of the candidate materials becomes much greater when aqueous corrosion processes initiate. The key parameters appear to be humidity, temperature, and surface condition; the experimental work aims to determine the interrelationship among these parameters. Thermogravimetric analysis (TGA) is a particularly sensitive technique for using a micro-analytical balance to measure very small changes in weight gain as a material reacts with the environment. G. Gdowski is the principal investigator; J. Estill and S. Gordon provide technical support.

A new furnace arrangement was integrated into the TGA apparatus. The manufacturer supplied furnace did not give an adequate temperature control within the reaction zone for the conduct of tests. The temperature varied by 15 to 20°C within the manufacturer specified reaction zone. With the new furnace arrangement, temperature variation is 1 to 2°C within a 5-cm reaction zone. Also with the new arrangement, the reaction zone is the low temperature region within the furnace, eliminating the problem of water condensation from high humidity air on other parts of the furnace.

It has been noticed that there is very low frequency noise on the signal from the TGA. An attempt is being made to find the source of this noise and then eliminate it. Also, mathematical manipulation of the data will be attempted to remove the noise from the signal.

Corrosion Sensor Development—Support to Large Block Test

The purpose of this activity is to develop sensors and methods to monitor atmospheric corrosion phenomena for prospective container materials, and also to investigate the rates and mechanisms of microbiologically induced corrosion (MIC). Past work has centered on measurements in the liquid phase. Relatively little work has been done, relevant to the Yucca Mountain Site Characterization Project, on the application of electrochemical methods (and other sensors) in the gas phase, which is a more realistic corrosion environment for the repository. Our current efforts center around the

development of microelectrode arrays for corrosion potential/rate measurements in the gas phase, initially to be used in the Large Block Test, and the use of the quartz crystal microbalance for studying MIC processes.

pH Sensing Electrode

Work continues on evaluating solid state iridium (IV) oxide pH sensors for application in the large block test. Iridium wire coated with iridium (IV) oxide has been prepared by electrolysis and will be used in evaluating polymeric coatings for ion-exchange and protection. Initial tests indicate that this electrode must be used with a high input impedance measuring circuit despite literature claims citing low impedance devices as being adequate.

Polymers may be modified by "quarternization" so that they become water soluble and electrically conductive. One such compound is poly (chloromethyl) styrene partially quarternized with triethylamine. Quarternary ammonium compounds are compounds in which there is a tetrasubstituted ammonium salt. They are commonly made from the reaction of a tertiary (i.e. a trisubstituted ammonia) amine with a halide (e.g. chloride) substituted compound. In the case of a partially quarternized poly(chloromethyl)styrene, the reaction with triethylamine occurs in connection with the chloromethyl sections of the polymer. The nitrogen in the amine attaches at the methyl and carries a positive charge balancing the negative charge on the chlorine. There are many chloromethyl groups along the polymer chain, and if not all of them are reacted, then the molecule is "partially quarternized". The resulting salt is now water soluble whereas the original polymer was not. The net result is that a polymer that is not soluble or miscible with water and not electrically conductive is modified so that it becomes water soluble, becomes ionic, and will support electrolytic conduction of electricity. These are desirable material properties for our use. On the negative side, adhesion becomes less than optimal.

This modified polymer is being evaluated as a coating to bridge the iridium oxide electrode and the reference chloride. An initial test consisted of refluxing the polymer with the amine in tetrahydrofuran for an hour. The resulting product was spread as a thin film on a glass slide and dried. The film was conductive with a marked decrease in resistance when exposed to humidity. As a coating over a silver/silver chloride wire electrode, the quarternized polymer did not interfere with the performance of the electrode. A sample of this material was submitted for infrared analysis, and the resulting spectrum indicated that the polymer had also undergone a significant degree of oxidation. This led to formation of a gel as the polymer aged. To avoid the unwanted oxidation, a second method of preparation was investigated. A sample of the polymer dissolved in tetrahydrofuran was cast on a salt plate, dried, and then soaked with the amine. On drying, the infrared spectrum was recorded; evidence of quarternization was detected in this room temperature reaction.

Corrosion Potential Measurements

Preliminary tests using a prototype probe indicated that corrosion potential could be determined in a humid atmosphere. However, the BEMCO environmental chamber failed due to a bad controller. A replacement controller has been ordered and installed and awaits calibration and tuning before work resumes in the chamber.

Quartz Crystal Microbalance/MIC

A quick test was conducted on the feasibility of growing cultures for researching MIC using the quartz crystal microbalance. Soil was suspended in excess water and a sheet of copper foil was exposed. According to the literature review, microorganisms should attach to the surface and establish colonies. This was confirmed by microscopic examination which revealed bacilli (unknown) and biofilm on the copper surface.

Crack Growth Tests (PACS OL232LFD, Activity E-20-18F)

The purpose of this work is to determine the stress corrosion cracking (SCC) susceptibility of candidate container materials under a variety of environmental, metallurgical, and mechanical stress conditions relevant to the repository. Stress corrosion is an important degradation mode that can affect both corrosion-allowance and corrosion-resistant materials. A sensitive crack growth measurement apparatus, which operates under the principle of measuring minute changes in the electrical resistance of the test specimen as a crack propagates, is in use at Argonne National Laboratory (ANL) to measure crack growth on pre-cracked compact tension fracture mechanics type of specimens. Principal Investigators at ANL are D. Diercks and J. Park. A similar unit is being commissioned at LLNL under the direction of E. Dalder, with the assistance of J. Estill and S. Gordon.

As stated in previous reports, all six of the alloys to be tested by ANL in this program (Titanium Grade 12, Hastelloy C-4, and Hastelloy C-22, as well as new heats of Incoloy 825, Type 304L SS, and Type 316L SS) have been purchased. The alloys are in the form of plate, and the chemical compositions of the alloys have been confirmed to conform to specifications. Four 1T-compact tension specimens were machined from each of the six materials. The compact tension specimens are being fatigue-cracked in air at room temperature under a cyclic load with triangular load shape, load ratio of R-0.1 to 0.25 and 1 Hz, to introduce a sharp starter crack before crack growth rate testing.

Fatigue precracking of the 1T-compact specimens continued. Eight specimens were completed for the precracking, two each from Titanium Grade 12 (Specimens T16-01 and T16-02), Hastelloy C-4 (Specimens 245-01 and 245-02), Hastelloy C-22 (Specimens 227-01 and 227-02), and Incoloy 825 (Specimens HH7-01 and HH7-02). Low-R cyclic crack growth rate tests will be initiated for Specimens T16-01, 245-02 and 227-02 in September.

The LLNL crack-growth measurement unit was down for much of August, while additional sheathed thermocouples were procured and installed in locations next to the three test-specimens. This was done to allow temperatures on each test-specimen to be measured directly, in the hope an "apparent" 40°C temperature difference between the inlet and outlet H_2O temperatures could be corrected by proper placement of the thermocouples near the samples. The crack-growth

measurement unit was sealed for operation on August 31, and warm-up to the test temperature of 60°C was begun.

A quality assurance audit of the ANL work, including that which supports the Metal Barrier Task, is scheduled for early September. E. Dalder will represent the Metal Barrier Task Leader.

Engineered Materials Characterization Report—EMCR (PACS OL232LFE)

The purpose of preparing the materials characterization report is to compile and synthesize information on the cogent properties of the candidate materials for the Waste Package and other Engineered Barrier System components. This report is planned to incorporate information on the important physical, mechanical, and chemical properties of the candidate materials, plus an outline of the long range and short range testing planned during ACD. Much of the long range testing plans were discussed in the Planning Documents section above. The Engineered Materials Characterization Report (EMCR) will serve as input to the Basis For Design document for Waste Package design and will provide a great deal of useful information.

D. Jones (UNR) and R. Van Konynenburg are working to complete a draft of the engineered materials characterization report by September 30.

1.2.2.3.3 Other Materials

This WBS element has not been funded in FY94.

On August 18 LLNL was visited by T. Murphy and J. Troxell of SCM Metal Products, Inc., and D. Peters of the Copper Development Association. The visitors gave an extensive and informative presentation on boron-containing powder-metallurgy copper and copper alloys for possible use as "Basket Materials" within the waste container for the purpose of criticality-control. The information obtained will be factored into the new "Basket Materials Task" in FY95.

1.2.2.3.4 Integrated Testing

This WBS element has been moved to WBS element 1.2.3.10.3.

1.2.2.3.5 Non-Metallic Barrier Concepts

(PACS OL235JGD and OL235KKA)

The purpose of the non-metallic barriers task is to characterize the behavior of non-metallic materials, such as ceramics, and to determine degradation rates and mechanisms, including the interaction between the barrier and the surrounding environment. The work in the non-metallic barriers task parallels that in the metallic barriers task. One of the multiple barriers of the waste package container may be fabricated from a non-metallic material. A primary objective of this task is determination of the feasibility of making a non-metallic barrier as part of a waste package.

K. Wilfinger's draft report entitled "Ceramic Package Fabrication for YMP Nuclear Waste Disposal" has completed internal technical review by R. Landingham, and comments are being incorporated. When the complete document is submitted to YMSCO, Milestone MOL57 will be complete.

1.2.2.4 Design, Fabrication, and Prototype Testing

1.2.2.4.3 Container/Waste Package Interface Analysis

This WBS element has not been funded in FY94.

1.2.3 SITE INVESTIGATIONS

1.2.3.1 Site Investigations Coordination and Planning

LLNL developed budget impact cases for A. Simmons (YMSCO). A reduction of 34% was made in the LLNL 1.2.3 (Geochemistry Team-managed portion) upload value.

1.2.3.2 Geology

1.2.3.2.1.2.1 Natural Analog of Hydrothermal Systems in Tuff

This WBS element has not been funded in FY94. The Study Plan will be deleted from the technical baseline, and its objective will be incorporated into Study Plans 8.3.4.2.4.1 and 8.3.1.20.1.1.

1.2.3.4 Geochemistry

1.2.3.4.2 Geochemical Modeling

This subtask is developing geochemical modeling software (EQ3/6) for analysis and simulation of interactions among water, rock, nuclear waste, and other repository components in the near-field environment, the altered zone, and the far-field environment. Work is continuing on EQ3/6 Version 8.0. In FY93, LLNL completed a major re-write of the software, incorporating major changes in the data structure in order to accommodate improvements in numerical methods and the addition of new functional capabilities. This included modifying the EQ6 code to utilize the auxiliary basis concept, thus allowing it to make reaction path calculations incorporating specified redox disequilibria. This capability is important to treating the metastable persistence of dissolved components such as sulfate, nitrate, and organics in laboratory and field settings. In FY94, LLNL is adding two additional capabilities to EQ3/6: (1) thermodynamic pressure corrections and (2) a generic ion-exchange model. In FY94, LLNL is also conducting an independent verification and validation (V&V) activity on EQ3/6 Version 7, which has already been distributed to various YMP participants for use in non-quality-affecting work only, pending certification.

The independent V&V activity for EQ3/6 Version 7 was completed in August. A baseline review was then conducted to ascertain and document the suitability of the software for certification (qualification) for use in quality-affecting work. The V&V activity found a few minor defects in Version 7.2a, the last version issued to YMP users for use in non-quality-affecting work only, pending certification. These did not adversely impact the suitability of the software for certification, and Version 7.2a was certified. This meets milestone MOL59. The minor defects are being fixed, and corrections will be issued as part of a Version 7.2b release (this version will be "born certified"). YMP users will be notified of the certification of Version 7.2a and the plan to issue Version 7.2b. The V&V report itself is being prepared for publication in summary form as a UCRL-ID report, along with a very lengthy supplement as a letter report. Other records related to the V&V are being prepared for submission to the LRC as records packages.

The work on incorporating thermodynamic pressure corrections was completed in August. Pressure corrections are implemented only if using a supporting data file which contains the necessary supporting data. The only data file presently supporting this capability is the new "SHV" data file, which is entirely based on SUPCRT92. It contains data grids for volume and enthalpy functions that correspond to those currently used for equilibrium constants. These grids represent the temperature dependence of these functions, along a standard pressure curve. The volume functions (standard partial molar volumes for strict basis species, standard partial molar volumes of reaction for all other species) are used to provide a first-order pressure correction to the equilibrium constants, which are represented on parallel data grids. The software is written to allow corrections of up to second order for the volume functions themselves, corresponding to corrections of up to third order for the equilibrium constants. The software is written to allow the enthalpy functions to be treated analogously to the volume functions. Although the enthalpy functions can theoretically be used to make temperature corrections to the equilibrium constants, they are not used for this purpose (the grid representation is used instead). The enthalpy functions will be used to track heat balances in boiling models to be developed in FY95 (see below); they have been added to the software at this time for the sake of efficiency.

The temperature grid used to represent equilibrium constants, volume functions, and enthalpy functions has been generalized in the software to allow variable grid parameters (e.g., an arbitrary number of temperature ranges and an arbitrary number of points in any range). Discussions are underway with the data base group to increase the upper limit of the temperature range of the SHV data file from 300°C to 400°C or higher, to better support analysis of experimental data and natural analog studies.

In the near-field environment, pressures are expected to remain relatively low (less than about 20 bars or so). Pressure corrections in this regime are practically nil except for reactions involving gas species. At present, EQ/6 offers limited treatment of gases, so the significance of such corrections in the near-field environment will have to be demonstrated at a later time, after the addition of boiling models in FY95. Pressure corrections are generally more important below the water table, increasing in importance with depth. Hydrostatic pressure increases by about 1 bar for every 10 m, or 100 bars per kilometer. Preliminary calculations suggest that the affects of pressure changes on the solubility of minerals such as calcite are significant in the 1-500 bar range (0-5 km depth below the water table), in line with expectations. These conditions are expected to be pertinent to the deeper parts of the altered zone and the far-field environment. They are also expected to be pertinent to the interpretation of natural analog studies (e.g., extrapolating to lower pressures as in the near-field environment).

Work on implementing the ion exchange capability is continuing and is expected to be completed by the end of September. This will complete planned code development for Version 8. A description of the differences between Version 8 and Version 7 is due as milestone MOL60 on September 30.

In FY95, LLNL will be adding boiling models to EQ3/6 (Version 9). This will include making use of the enthalpy function data to track heat balances. Also, an independent V&V activity will be conducted on EQ3/6 Version 8.

1.2.3.5 Drilling

1.2.3.5.2.2 Engineering, Design, and Drilling Support

No significant activity.

1.2.3.10 Altered Zone Characterization

1.2.3.10.1 Characterization Techniques for the Altered Zone

No significant activity.

1.2.3.10.2 Characterization of Thermal Effects on the Altered Zone Performance

Experiments to examine rock-water interaction in relevant lithologic units continue.

1.2.3.10.3 Integrated Testing

1.2.3.10.3.1 Integrated Radionuclide Release: Tests and Models

Activity will be discussed in a later monthly progress report.

1.2.3.10.3.2 Thermodynamic Data Determination

Activity will be discussed in a later monthly progress report.

1.2.3.11 Integrated Geophysical Testing for Site Characterization

1.2.3.11.3 Geophysics—ESF Support, Subsurface Geophysical Testing

No significant activity. The work will resume when the capital and non-capital procurements have been received, which is expected in September.

1.2.3.12 Waste Package Environment Testing

This WBS element was created from WBS element 1.2.2.2. Reporting and PACS have been converted to the new system, and funding has been moved from WBS 1.2.2.

1.2.3.12.1 Chemical and Mineralogical Properties of the Waste Package Environment

Activity will be discussed in a later monthly progress report.

1.2.3.12.2 Hydrologic Properties of the Waste Package Environment

Draft Study Plan 8.3.4.2.4.2 has been revised in response to reviewers' comments. The changes are being incorporated and will be returned to YMSCO in September.

Thermo-Hydrological Calculations

In order to augment the thermo-hydrological calculation support of the thermal loading systems study, LLNL has been conducting the calculations in the near-field/altered zone hydrology task with the same set of thermal loading assumptions (see Sec. 1.2.1.5). In August, we investigated

- The impact of an optimized, nonuniform areal mass loading (AML) distribution on generating more uniform subambient relative humidity conditions.
- The impact of enhanced gas-phase diffusion on these optimized AML scenarios.
- The applicability of the equivalent continuum model to representing fracture-matrix behavior under repository thermal loads.

The calculations described in this (and previous) progress reports assume the repository to be 343.1 m below the ground surface (i.e., 343.1-m-thick overburden). In Sec. 1.2.1.5, we discuss the impact of the overburden thickness on thermo-hydrological behavior.

Analysis of the Impact of an Optimized AML Distribution and Enhanced Gas-Phase Diffusion on Temperature and Relative Humidity Conditions in the Repository

In past progress reports, we have described the temperature *T* and relative humidity *RH* conditions throughout the repository (center to edge), primarily for cases with a uniform-AML distribution. Table 1 (in Sec. 1.2.1.5) summarizes the *T* and *RH* conditions for the uniform-AML cases. For uniform-AML cases, we have noted the following in past progress reports:

- The duration of sub-ambient *RH* conditions is greatest for high-AML cases, decreasing with AML.
- The temperature associated with a given value of *RH* decreases with increasing AML.
- The duration of sub-ambient *RH* conditions is greatest in the inner 50% of the repository, decreasing as the repository edge is approached.
- The temperature associated with a given value of *RH* increases as the repository edge is approached.

The outer perimeter of high, uniform-AML repositories (e.g., 110.5 MTU/acre) exhibits *T–RH* behavior that is characteristic of the inner 50% of intermediate, uniform-AML repositories (e.g., 55.3 MTU/acre). These *T–RH* results are calculated with the smeared-heat-source, disk-shaped model of the repository. Therefore, *RH* is determined by temperature and liquid saturation conditions that are effectively averaged from the midline of the emplacement drift to the midline of the pillar separating the emplacement drifts. Local conditions close to the WPs will be hotter and drier than average conditions, particularly during the first 100 yr. It should also be noted that thermo-hydrological heterogeneity and variability in the heat output among the WPs will cause local behavior to deviate from average behavior.

In August, we considered an optimized, nonuniform-AML distribution that was discussed in the February and March progress reports (in Sec. 1.2.1.5), with an average AML of 128.4 MTU/acre. The AML in the inner 75% of the repository has a uniform AML of 110.5 MTU/acre, while for the outer 25%, it is nonuniform, increasing as the outer perimeter is approached, with an average AML of 180.2 MTU/acre over the outer 25%. Effectively, the nonuniform 128.4-MTU/acre case is the uniform 110.5-MTU/acre case, with the local AML of the outer 25% of the repository increased by 63%. This month we applied the same normalized AML distribution scheme to the uniform 55.3, 70, 83.4, 110.5, and 150 MTU/acre cases, obtaining average AMLs of 62.4, 83.1, 96.9, 128.4, and 174.3 MTU/acre. For example, the inner 75% of the nonuniform 62.4-MTU/acre case has a uniform AML of 55.3 MTU/acre, while the outer 25% has a nonuniform-AML distribution with an average of 90.2 MTU/acre. The 174.3-MTU/acre case assumes 40-yr-old SNF, while all other cases assume the reference YFF(10), 22.5-yr-old, SNF. For this suite of

optimized, nonuniform-AML cases, we considered the case of "nominal" binary gas-phase diffusion (Table 4), where the binary, gas-phase diffusion tortuosity factor $t_{eff} = 0.2$, and the case of "enhanced" binary gas-phase diffusion (Table 5), where $t_{eff} = 4.0$ (see the January 1994 progress report for the definition of t_{eff}).

Table 4. Gas-phase diffusion tortuosity factor $t_{eff} = 0.2$.
Time required to attain indicated relative humidity at various repository locations, and temperature when that value of relative humidity is attained for an optimized AML distribution and $k_b = 280$ millidarcy.
Locations are identified as the percentage of the repository area enclosed; 0% corresponds to the repository center and 100% corresponds to the outer perimeter.

Table 4a. Average AML = 62.4 MTU/acre, 22.5-yr-old SNF.

	Time required to attain indicated relative humidity (yr)				Temperature when indicated relative humidity is attained (°C)			
Repository area enclosed (%)	70%	80%	90%	95%	70%	80%	90%	95%
50	980	2160	4720	6650	106	95	75	69
75	1420	3150	6990	10,020	102	80	65	60
90	1690	3160	5920	8350	92	76	66	61
97	1030	1520	2400	3380	98	88	77	70

Table 4b. Average AML = 83.1 MTU/acre, 22.5-yr-old SNF.

	Time required to attain indicated relative humidity (yr)				Temperature when indicated relative humidity is attained (°C)			
Repository area enclosed (%)	70%	80%	90%	95%	70%	80%	90%	95%
50	4140	11,300	21,940	30,770	89	66	52	46
75	4050	10,190	18,570	28,450	85	66	53	46
90	3220	5,870	9,320	12,160	85	73	65	60
97	1720	2,490	3,770	4,830	98	87	77	73

Table 4c. Average AML = 96.9 MTU/acre, 22.5-yr-old SNF.

	Time required to attain indicated relative humidity (yr)				Temperature when indicated relative humidity is attained (°C)			
Repository area enclosed (%)	70%	80%	90%	95%	70%	80%	90%	95%
50	10,420	22,250	36,190	46,450	73	55	45	40
75	8,420	17,680	29,290	37,590	75	58	48	43
90	5,400	9,200	13,860	18,720	81	70	61	55
97	2,710	4,060	6,030	7,950	93	83	75	70

Table 4d. Average AML = 128.4 MTU/acre, 22.5-yr-old SNF.

	Time required to attain indicated relative humidity (yr)				Temperature when indicated relative humidity is attained (°C)			
Repository area enclosed (%)	70%	80%	90%	95%	70%	80%	90%	95%
50	17,860	32,330	49,080	61,000	67	51	43	39
75	14,820	25,470	37,760	44,290	69	55	47	44
90	10,470	15,280	21,040	28,070	76	66	58	51
97	6330	8,830	11,710	14,380	85	77	70	65

Table 4e. Average AML = 174.3 MTU/acre, 40-yr-old SNF.

	Time required to attain indicated relative humidity (yr)				Temperature when indicated relative humidity is attained (°C)			
Repository area enclosed (%)	70%	80%	90%	95%	70%	80%	90%	95%
50	19,210	33,160	49,360	60,360	73	55	46	42
75	17,560	26,530	37,380	44,670	73	61	51	47
90	14,150	18,750	26,680	31,230	77	68	58	54
97	10,670	13,550	17,210	19,430	82	75	68	64

Table 5. Gas-phase tortuosity factor $t_{eff} = 4.0$.
Time required to attain indicated relative humidity at various repository locations, and temperature when that value of relative humidity is attained, for an optimized AML distribution, and $k_b = 280$ millidarcy.
Locations are identified as the percentage of the repository area enclosed; 0% corresponds to the repository center and 100% corresponds to the outer perimeter.

Table 5a. Average AML = 62.4 MTU/acre, 22.5-yr-old SNF.

Percentage of repository area enclosed (%)	Time required to attain indicated relative humidity (yr)				Temperature when indicated relative humidity is attained (°C)			
	70%	80%	90%	95%	70%	80%	90%	95%
50	940	2330	15,550	26,400	106	90	56	42
75	1460	3650	15,750	32,640	98	74	50	39
90	1950	4690	16,820	29,950	86	66	48	39
97	1320	2450	82,90	17,640	90	75	57	46

Table 5b. Average AML = 83.1 MTU/acre, 22.5-yr-old SNF.

Percentage of repository area enclosed (%)	Time required to attain indicated relative humidity (yr)				Temperature when indicated relative humidity is attained (°C)			
	70%	80%	90%	95%	70%	80%	90%	95%
50	5020	10,830	27,460	48,300	79	63	45	37
75	4650	10,580	26,940	46,380	78	62	45	37
90	3880	9,740	23,390	36,050	78	61	46	40
97	2280	4,960	14,310	24,530	88	70	53	45

Table 5c. Average AML = 96.9 MTU/acre, 22.5-yr-old SNF.

Percentage of repository area enclosed (%)	Time required to attain indicated relative humidity (yr)				Temperature when indicated relative humidity is attained (°C)			
	70%	80%	90%	95%	70%	80%	90%	95%
50	10,550	18,600	40,810	72,170	68	56	41	35
75	9290	17,040	36,990	59,450	68	56	42	36
90	7790	15,110	29,780	41,870	69	57	44	39
97	4460	10,270	21,160	29,610	77	62	49	43

Table 5d. Average AML = 128.4 MTU/acre, 22.5-yr-old SNF.

Percentage of repository area enclosed (%)	Time required to attain indicated relative humidity (yr)				Temperature when indicated relative humidity is attained (°C)			
	70%	80%	90%	95%	70%	80%	90%	95%
50	17,300	28,180	54,170	87,660	65	53	40	35
75	16,150	26,490	47,340	69,050	64	53	42	37
90	14,620	24,090	39,030	49,660	64	53	44	40
97	11,650	18,900	30,840	41,150	67	56	47	42

Table 5e. Average AML = 174.3 MTU/acre, 40-yr-old SNF.

Percentage of repository area enclosed (%)	Time required to attain indicated relative humidity (yr)				Temperature when indicated relative humidity is attained (°C)			
	70%	80%	90%	95%	70%	80%	90%	95%
50	22,990	33,190	59,600	90,040	65	54	42	36
75	21,260	30,970	52,710	72,870	64	54	43	38
90	19,420	28,460	41,960	53,600	64	55	46	42
97	16,420	23,860	34,090	41,440	67	58	49	46

A comparison of Table 4a with Table 1a (in Sec. 1.2.1.5) clearly shows that an optimized, nonuniform-AML distribution can benefit intermediate AMLs. While the uniform 55.3-MTU/acre case has a negligible reduction in *RH* for the outer 10% of the repository, the nonuniform, 62.4-

MTU/acre case has a moderately substantial period of sub-ambient *RH* conditions (Table 4a). A comparison of Table 4b with Table 1b (in Sec. 1.2.1.5) shows that, in addition to substantially improving *T–RH* behavior for the outer 10% of the repository, *T–RH* behavior is also improved for the inner 90% of the repository. The improvement for the outer 10% of the repository is also applicable to high AMLs. A comparison of Table 6a with Table 3a (in Sec. 1.2.1.5) also shows the benefits of utilizing an optimized, nonuniform-AML distribution during the above-boiling period. The optimized, nonuniform-AML cases result in:

- More uniform distribution of the duration of the boiling period t_{bp}.
- Lower values of *RH* at the end of the boiling period, particularly for the outer 25% of the repository.

Table 6. Nonuniform (optimized) AML distributions.
Duration of boiling at various repository locations, and relative humidity attained at the end of the boiling period, k_b = 280 millidarcy, and a repository depth of 343.1 m (reference case). Fuel age is 22.5 yr for the four lower AMLs and 40 yr for the highest AML.
Locations are identified as the percentage of the repository area enclosed, with 0 percent corresponding to the repository center, and 100 percent corresponding to the outer perimeter.

Table 6a. Gas-phase diffusion tortuosity factor t_{eff} = 0.2.

Repository area enclosed (%)	Duration of boiling period (yr) and relative humidity (%) at end of boiling period for indicated average AMLs									
	62.4 MTU/acre		83.1 MTU/acre		96.9 MTU/acre		128.4 MTU/acre		174.3 MTU/acre	
50	2040 yr	79%	3300 yr	67%	4400 yr	54%	6980 yr	44%	10,810 yr	52%
75	1770 yr	73%	2710 yr	65%	3720 yr	55%	5900 yr	44%	9,190 yr	49%
90	1470 yr	67%	2250 yr	63%	2960 yr	59%	4790 yr	50%	7,990 yr	50%
97	1120 yr	72%	1820 yr	71%	2460 yr	68%	3990 yr	58%	6,570 yr	54%

Table 6b. t_{eff} = 4.0.

Repository area enclosed (%)	Duration of boiling period (yr) and relative humidity (%) at end of boiling period for indicated average AMLs									
	62.4 MTU/acre		83.1 MTU/acre		96.9 MTU/acre		128.4 MTU/acre		174.3 MTU/acre	
50	1810 yr	77%	2860 yr	62%	3660 yr	49%	5530 yr	39%	9420 yr	41%
75	1590 yr	71%	2470 yr	60%	3210 yr	50%	4740 yr	39%	7990 yr	40%
90	1350 yr	63%	2130 yr	60%	2730 yr	54%	4030 yr	42%	6770 yr	41%
97	1060 yr	65%	1770 yr	64%	2330 yr	60%	3520 yr	48%	5740 yr	43%

As was observed for the uniform-AML cases, the temperature associated with a given value of *RH* for the nonuniform-AML cases decreases with increasing AML (Table 4). As in the uniform-AML cases, this trend of decreasing temperature with increasing AML levels off at about 128.4 MTU/acre. In the May progress report, we observed for the uniform-AML cases that this trend levels off for the inner 75% of the repository at about 110.5 MTU/acre, while for the outer 25%, the trend continues for higher AMLs. Also, the incremental benefit of increasing the nonuniform-AML distribution from an average of 96.9 to 128.4 MTU/acre is greater than the improvement in *T–RH* behavior obtained between 128.4 and 174.3 MTU/acre. In other words, increasing the average AML above 128.4 MTU/acre yields somewhat diminishing returns in *T–RH* behavior.

One of the major objectives of the optimized, nonuniform-AML distribution is to drive the entire repository environment to more uniform *T–RH* conditions. However, it should be recognized that large-scale heterogeneity in hydrological properties (e.g., the distribution of bulk permeability k_b) will cause local deviations from averaged *T–RH* behavior, particularly during the post-boiling period, as the reduced-*RH* zone re-wets heterogeneously to ambient (humid) conditions. A primary motivation for generating more uniform, persistent, above-boiling conditions (and reduced-*RH*

conditions), is to enhance the period of substantially complete containment (SCC). Such performance enhancement due to emplacement geometry is one way to substantiate the controlled design assumption that a given waste package design will meet the SCC requirements.

A second motivation for generating more uniform, persistent reduced-*RH* conditions is to enhance performance with respect to the EBS controlled release regulatory requirement. Of the two major environmental factors affecting the rate of aqueous corrosion (*T* and *RH* on the WP surface), variations in *T* within the repository will tend to even out far earlier than variations in *RH*. During the period of substantial thermal perturbation of *RH* conditions (from ambient), *RH* conditions will never be more uniform than during the above-boiling period, while during the post-boiling period, deviations in local *RH* behavior from average behavior will tend to grow (as certain regions of the repository re-wet earlier than others), and then eventually dissipate as the entire repository has finally re-wetted to ambient (humid) conditions. Depending on what is learned from site characterization and *in situ* heater testing, the period of substantial thermal perturbation of *RH* conditions will last from several times to perhaps ten times the boiling period. Some regions may continue to have sub-ambient *RH* conditions for a period twenty times the boiling period. Deviations will inevitably occur from the mean time to re-wet to humid conditions (with respect to aqueous corrosion) due either to proximity to the repository edge or to how heterogeneity will influence re-wetting behavior. Therefore, increasing the mean time to re-wet to humid conditions will tend to result in generally lower temperatures once relatively humid conditions have been restored, and perhaps more important for controlled release, in a greater temporal dispersion in the rate of aqueous corrosion rates from place to place within the repository. Dispersion in aqueous corrosion rates will tend to result in temporal dispersion of the distribution of WP failure times, thereby temporally dispersing the potential source term for radionuclide transport. A dispersion in WP failure times would be more likely to meet the EBS controlled release requirement than a situation with a narrow distribution in WP failure times. This observation would be particularly true if the narrow distribution occurs at relatively early time.

The results summarized in Tables 4 and 6a are for the case of "nominal" binary gas-phase diffusion, with $t_{eff} = 0.2$. We repeated the calculations for the same suite of AMLs with $t_{eff} = 4.0$, which may be considered to be a case of "enhanced" binary gas-phase diffusion. A comparison of Tables 4 and 5 shows that enhanced binary gas-phase diffusion has the effect of

- Increasing the time to re-wet to *RH* = 70, 80, 90, and 95% for the outer 25% of the repository, with the effect being greatest at the outer 10%.
- Substantially increasing the time to re-wet to *RH* = 90 and 95% for the entire repository.
- Lowering the temperature associated with a given *RH*, particularly for the outer 10% of the repository and for *RH* = 90 and 95%.

The last observation is particularly applicable to high AMLs.

A comparison of Tables 6a and 6b shows that enhanced binary diffusion has the effect of

- Decreasing t_{bp}.
- Lowering the value of *RH* at the end of the boiling period, particularly for the outer 10% of the repository.

The first observation arises because the enhanced diffusion of water vapor away from the heat source contributes to latent heat transport, thereby enhancing the cooling of the repository. The second observation causes more uniform *RH* conditions to occur throughout the repository. Therefore, the combination of the optimized, nonuniform-AML distribution and enhanced gas-phase diffusion results in very uniform *RH* conditions in the repository during the boiling period.

In July, we observed that enhanced vapor diffusion enhances the re-wetting rate only where the advective liquid-phase re-wetting rate is already relatively slow (i.e., the cases with slow liquid-phase re-wetting rates and at the center of the repository). Enhanced vapor diffusion reduces the overall re-wetting rate where the advective liquid-phase re-wetting rate is fastest. Therefore, enhanced gas-phase diffusion may be thought to function somewhat as an equalizer of *T–RH* conditions, countering some of the effects of heating variability and heterogeneity in various hydrological properties. A comparison of Tables 4 and 5 clearly shows the "equalizing" effect of enhanced vapor diffusion on *T–RH* conditions. For example, between the 50 and 97% repository location, there is a 2.8-fold difference in the time to re-wet to $RH = 70\%$ for the 128.4-MTU/acre, nominal vapor diffusion case (Table 4d), while there is only a 1.5-fold difference in the enhanced diffusion case (Table 5d). Between the 50 and 97% repository location, there is an 18°C range in temperatures associated with $RH = 70\%$ (Table 4d) for the nominal vapor diffusion case, while for the enhanced vapor diffusion case there is only a 2°C range in temperature (Table 5d). Clearly, it will be extremely important to determine, in laboratory and *in situ* heater tests, the degree to which vapor diffusion may be enhanced at Yucca Mountain. As discussed in the March progress report, determining the extent of enhanced vapor diffusion is also critical to quantifying the diffusive loss of moisture to the atmosphere under both ambient and repository-disturbed conditions.

A Comparison of the Equivalent Continuum Model (ECM) with the Fracture-Matrix Model (FMM) for Repository-Heat-Driven Hydrothermal Flow

In past work, LLNL has investigated the applicability of the equivalent continuum model (ECM) to representing nonequilibrium fracture-matrix flow. For ambient conditions, we have found that the ECM cannot represent natural infiltration generated by intense transient episodes of recharge. We have also found that it cannot be used to explain the measurement of anomalously high liquid saturations in the vitric nonwelded units such as the PTn and Chnv.

In comparing the ECM and the nonequilibrium fracture-matrix model (FMM) in the modeling analysis of the G-Tunnel heater test, we found that the ECM did very well in representing the temperature distribution and the liquid saturations in the dry-out zone; however, it could not represent the apparent condensate shedding around the boiling zone. Although no liquid saturation buildup was observed during the G-Tunnel heater test, the ECM predicted a buildup of liquid saturation in the condensation zone. The magnitude of the buildup can be estimated from the average condensate generated per meter of fracture during the 128-day, full-power heating stage, based on the net dry-out volume and three fractures per meter. A condensate flux of about 300 milliliter/day per meter of fracture is estimated.

For the ECM models used for the Thermal Loading Systems Study, we conducted a comparison with the FMM for an AML of 110.5 MTU/acre. Both the ECM and the FMM used one-dimensional vertical columns through the repository horizon. These models thus assume an infinite area repository. However, because our comparison is for the first 80 yr, during which time edge cooling effects have not penetrated far into the repository area, this comparison is applicable to much of the repository area. Throughout the 80-yr simulation, there is outstanding agreement in both the temperature and liquid saturation profiles predicted by the ECM and the FMM. Moreover, agreement between the two models in predicting the *RH* history at the repository is outstanding. The two models predict almost identical liquid saturation profiles in the sub-boiling region (above the upper condensate zone and below the lower condensate zone) as well as in the zone of condensate buildup, including the refluxing zone above the boiling zone. In the driest part of the dry-out zone, the FMM predicts slightly larger liquid saturation than the ECM; however, the agreement in the *RH* behavior is outstanding. We focused our comparison on early time because

this is when condensate flow rates are greatest, and therefore have the greatest potential of being out of equilibrium with the matrix. For comparison with the G-tunnel heater test, the condensate flow rate in the fracture at 80 yr is 15 milliliter/day per meter of fracture for the 110.5 MTU/acre case, which is only one-twentieth of the conservative estimate for that test.

We plan additional comparisons between the ECM and the FMM for larger fracture spacing and various matrix properties in order to identify conditions for which disequilibrium between fracture and matrix behavior causes the ECM to deviate from a discrete representation of fracture-matrix interaction. We are interested in identifying fracture densities for which dry-out in the matrix lags substantially behind dry-out along fractures, thereby causing the ECM to overpredict dry-out behavior. In particular, we are interested in identifying when the fracture density is sparse enough to cause *RH* conditions in the FMM to become significantly more humid than that predicted by the ECM. We also plan to examine the effect of binary vapor diffusion on nonequilibrium fracture-matrix behavior.

Laboratory Experiments

Electrical Impedance as a Function of Moisture Content

We completed the preparation of more samples from the G-4 hole and the large block test (LBT) cores to complete the measurements at 95°C. These samples have been dried and are being saturated to determine their porosity before being used for the electrical conductivity measurements. We continued utilizing the complex nonlinear least square method to analyze the data. The parameters derived from these fits can distinguish different phases of the water wetting/drying process.

Characteristic Curves of Tuff

For the experiment of determining the moisture retention curve and one-dimensional imbibition using G-4 core, we continued the moisture retention experiments at high temperatures. Measurements at 95°C in the drying phase continued. The samples are at 95°C and 60% relative humidity.

The Effect of Confining Pressure on Fracture Healing

We continued the experiment to determine the effect of confining pressure on fracture healing, as observed previously by Lin and Daily. A fractured Topopah Spring tuff sample from the G-4 hole is used. The sample is at an effective pressure of 2.5 MPa (3.0 MPa confining pressure and 0.5 MPa pore pressure), and it was heated to 150°C and then cooled to 100°C. The permeability decreased by about 50% during heating from 25°C to 150°C.

1.2.3.12.3 Mechanical Attributes of the Waste Package Environment

Activity will be discussed in a later report.

1.2.3.12.4 Engineered Barrier System (EBS) Field Tests

J. Blink D. Wilder, and W. Lin attended the ESF Test Planning meeting in Las Vegas on August 23. The meeting was hosted by the Test Coordination Office. Several options for heater tests were discussed.

Revisions to the Engineered Barrier System Field Tests (EBSFT) Study Plan (8.3.4.2.4.4) are in progress based on the comment resolution meeting.

Large Block Test (LBT)

Matrix Bulk Porosity

The determination of porosity using the wet-dry method continued. These samples have been dried and are being saturated.

Fracture Mapping

The evaluation of Earth Vision and other software as a tool to display the fracture data of the large block in 3-D continued. The fracture map of the top of the block has been digitized.

Excavation

The excavation work has been completed. The sampling of the small blocks to be used in the laboratory tests has begun. The sampling is expected to be completed early in September. The blocks will be sent to Nevada Neanderthal Stone (NNS) in Beatty, Nevada to be cut into smaller blocks so that they can be machined in the sample preparation facility at LLNL. NNS personnel have been trained to LLNL quality procedures.

Initial Moisture Content

The neutron logging data obtained from some of the vertical holes have been reduced, based on the LLNL calibration data of the neutron tool. The saturation levels of the block were between 60 and 80% at the time of the measurement.

Small samples of tuff obtained from Fran Ridge, for estimating the initial moisture content, were dried and are being saturated.

Small Block Tests in the Laboratory

Tests under a 5-MPa stress continued on the performance of the Kapton heaters (to be used as guard heaters for the large block and as heaters for the small block experiments), the potential insulation materials, and the thermal controller for the guard heaters.

X-ray imaging to determine water saturation has begun. A small block of 2.5 x 10 x 10 cm of Topopah Spring tuff from Fran Ridge, with a saw cut in the middle, has undergone a dry, background X-ray testing. Water doped with KI was added to the top of the sample and radiographs are being taken as a function of time to try to determine the distribution of water content. The water is slowly imbibing along the saw cut and into the matrix.

The Load Retaining Frame

Engineering analysis of the proposed modifications to retrofit the frame was completed. The load requirements for the anchor bolts have been determined. The results have been transmitted to RSN for designing the anchoring system.

Eight side sections of the frame have arrived at LLNL, and the welding has begun. The other four side sections are being completed by the vendor.

Loading Devices

The engineering design of the bladder support/housing devices continued. The procurement for bladders to be used to load the block has been prepared.

Pre-test Calculation

The first draft of a progress report on the scoping pre-test calculations was completed. The report will be issued in September.

Other Items

Procurement of instruments is ongoing. An integrated DOE contractor order (ICO) for calibrating the instruments was set up with EG&G.

1.2.3.12.5 Characterization of the Effects of Man-Made Materials on Chemical & Mineralogical Changes in the Post-Emplacement Environment

Activity will be discussed in a later monthly progress report.

1.2.5 REGULATORY

1.2.5.1 Regulatory Coordination and Planning

No significant activity.

1.2.5.2 Licensing

1.2.5.2.2 Site Characterization Program

J. Blink was host on August 10 at the Large Block Test Site for Dr. Ed Cording, an NWTRB member, and R. McFarland of the NWTRB staff.

J. Blink attended the planning meeting in Las Vegas on August 11 for the upcoming NWTRB meeting on groundwater travel time. D. Chesnut participated via conference call.

1.2.5.3 Technical Data Management

1.2.5.3.4 Geologic and Engineering Materials Bibliography of Chemical Species (GEMBOCHS)

Activity will be discussed in a later monthly progress report.

1.2.5.3.5 Technical Data Base Input

Sixteen TDIFs were entered into the ATDT system in August.

1.2.5.4 Performance Assessment

1.2.5.4.2 Waste Package Performance Assessment

A statistical study of the TSPA '93 data has been conducted to understand the TSPA model's parameters and repository performance. The TSPA analysis modeled the performance of four different repository designs having two different emplacement modes and two probability distributions over the performance of each design, based on the probability distributions of 98 input parameters. The statistical analysis identified parameters that are important in predicting repository performance and studied the underlying reasons for the differences in performance of the four designs.

The study has been conducted in four major parts:

1) Parameters were identified which influence repository performance. An evaluation was made to determine if some parameters may affect the performance of one design more than others.
2) Performance of the four designs was compared to identify the particular mechanisms that account for the difference in their behavior.
3) A reduced form model of the unsaturated zone releases was developed for the in-drift 114 kW/acre design. The reduced form model uses just a few of the parameters, yet is effective at predicting releases. It provides quantitative confirmation of the degree to which the model behavior is governed by a small set of parameters.
4) The releases from the engineered barrier system were studied to evaluate the extent to which each of the EBS related parameters influenced EBS performance.

An initial draft of the study has been completed and is undergoing informal review. It is expected that a final draft will be completed by the end of September.

1.2.5.5. Special Projects

1.2.5.5.1 Integrated Test Evaluation (ITE)

This activity has not been funded in FY94.

1.2.5.5.2 Energy Policy Act Support

No significant activity.

1.2.9 PROJECT MANAGEMENT

1.2.9.1 Management and Coordination

1.2.9.1.2 Technical Project Office Management

W. Clarke participated in the Blue Team Review of the OMB 5-year submission on August 14. J. Blink participated in the Blue Team Reviews on August 15 and 29.

W. Clarke presented the LLNL FY94 budget and progress status in Las Vegas on August 19. J. Blink and J. Podobnik also attended.

J. Blink was recognized by the DOE-NV Manager for his contributions to Public Outreach.

1.2.9.2 Project Control

1.2.9.2.2 Participant Project Control

Actual schedule progress and costs were submitted to the PACS reporting system via the PACS workstation. Variance analysis explanations were developed.

Preparation for the September upload of FY95 PACS planning began.

1.2.11 QUALITY ASSURANCE

Activity will be discussed in a later monthly progress report.

1.2.12 INFORMATION MANAGEMENT

1.2.12.2 Records Management

1.2.12.2.2 Local Records Center Operations (LRC)

LLNL-YMP Document Control issued one revision and no change notices. Follow up continues on previously distributed documents.

1.2.12.2.3 Participant Records Management

A total of 177 items were logged into the LLNL-YMP tracking system. This includes eight records/records packages that were processed through to the CRF. Sixteen action items were closed in August.

1.2.12.2.5 Document Control

LLNL received no funding under this WBS element for FY94. Work performed to complete LLNL's obligation in this WBS element is funded under WBS 1.2.12.2.2.

1.2.13.2 SAFETY AND OCCUPATIONAL HEALTH

1.2.13.2.5 Occupational Safety and Health

LLNL was notified of an ES&H audit of its NTS-YMP activities; the audit will be conducted during the week of September 26.

1.2.15 SUPPORT SERVICES

1.2.15.2 Administrative Support

Preparation began on compilation of the LLNL input to PR-11.

1.2.15.3 Yucca Mountain Site Characterization Project (YMP) Support for the Training Mission

Currently there are 113 participants on the project who are to be trained and/or tracked. Seven new individuals were added and one individual left the project in August.

The new training database program has been completed and installed. Data entry of all the information stored on the old system is in progress. This activity should be completed by the end of October.

T. Wolery conducted classroom training for 16 participants on Quality Procedure (QP) 3.2, Revision 2, Software Quality Assurance. This QP has replaced nine software technical implementation procedures.

J. Blink provided a Yucca Mountain QA orientation to four employees of Nevada Neanderthal Stone (NNS) in Beatty Nevada on August 10. He also provided training on three quality procedures to be used by these employees. NNS will work to LLNL-YMP QA procedures for this work. They are cutting laboratory samples from boulders taken at the Fran Ridge Large Block Test site. The samples will meet all QA requirements.

LLNL PROJECT STATUS REPORT EXTERNAL DISTRIBUTION
August 1994

PRELIMINARY STAMP
Dr. J. Bates Chemical Technology
Argonne National Laboratory
9700 S. Cass Avenue
Argonne, Illinois 60439

H. Benton
M&O, M/S 423
101 Convention Center Drive
Las Vegas, NV 89109

A. Berusch (RW-20)
OCRWM
Forrestal Building
Washington, DC 20585

M. Bishop
YMSCO
US Department of Energy
101 Convention Center Drive
Las Vegas, NV

M. Blanchard
YMSCO
Department of Energy
P.O. Box 98518
Las Vegas, Nevad 89193-8518

J. Blink
LLNL/Las Vegas
101 Convention Center Drive, Suite 880
Las Vegas, NV 89109

S. Bodnar
TRW, M/S 423
101 Convention Center Drive
Las Vegas, Nevada 89109-2005

B. Bodvarsson
LBL/Earth Sciences
Bldg. 50 E
1 Cyclotron Road
Berkeley, CA 94720

M. Brodeur
Science Applications Int'l Corp.
101 Convention Center Dr., #407
Las Vegas, NV 89109-2005

S. Brocoum
YMSCO
101 Convention Center Dr.
Las Vegas, NV 89109

J. Canepa
Los Alamos National Laboratory
P.O. Box 1663/N-5, MS J521
Los Alamos, NM 87545

P. Cloke
Science Applications Int'l Corp.
101 Convention Center Dr., #407
Las Vegas, NV 89109-2005

C. Conner
DOE, RW-133
1000 Independence Ave., SW
Washington, DC 20585

G. Cook
YMSCO
Department of Energy
P.O. Box 98518
Las Vegas, NV 89193-8518

W. Dixon
YMSCO
Department of Energy
P.O. Box 98518
Las Vegas, NV 89193-8518

T. Doering
M&O
101 Convention Center Dr., MS 423
Las Vegas, NV 89109

J. Dyer
YMSCO
Department of Energy
P.O. Box 98518
Las Vegas, NV 89193-8518

PRELIMINARY STAMP
R. Einziger
Battelle-Pacific Northwest
P.O. Box 999/MS P714
Richland, WA 99352

R. Fish
M&O
101 Convention Center Dr., M/S 423
Las Vegas, NV 89109

L. Foust
Technical Project Officer
CRWMS M&O, M/S 423
101 Convention Center Dr.
Las Vegas, NV 89109

A. Gil
YMSCO
Department of Energy
P.O. Box 98518
Las Vegas, NV 89193-8518

R. Green
Southwest Research Institute
6220 Culebra Rd.
San Antonio, TX 78238-5166

L. Hayes
U.S. Geological Survey
Box 25046/MS 425
Denver Federal Center
Denver, CO 80225

R. Hughey
Nuclear Energy Division
US DOE/OAK
1301 Clay St., Rm. 700-N
Oakland, CA 94612

N. Jones
M&O
101 Convention Ctr. Dr., M/S 423
Las Vegas, Nevada 89109

S. Kennedy
OCRWM
Forrestal Bldg.
Wash., D.C. 20585

V. Iorii
YMSCO
Department of Energy
P.O. Box 98518
Las Vegas, Nevada 89193-8518

C. Johnson
M&O
101 Convention Center Dr. M/S 423
Las Vegas, NV 89109

S. Jones
YMSCO
Department of Energy
101 Convention Center Dr.
Las Vegas, NV 89109

N. White (3)
Nuclear Regulatory Commission
301 E. Stewart Ave. #203
Las Vegas, NV 89101

H. Kalia
Los Alamos National Laboratory
101 Convention Center Dr., Suite 820
Las Vegas, NV 89109

PRELIMINARY STAMP
S. Marschman, P7-14
Battelle, Pacific Northwest
P.O. Box 999
Richland, WA 99352

M. Martin
TRW, M/S 423
101 Convention Center Dr.
Las Vegas, NV 89109-2005

S. Nelson
M&O
101 Convention Center Dr., M/S 423
Las Vegas, NV 89109

R. Robertson
TRW-Metro Place
2650 Park Tower Dr., Suite 800
Vienna, VA 22180

D. Rogers
M&O
101 Convention Center Dr., M/S 423
Las Vegas, NV 89109

S. Saterlie
M&O
101 Convention Center Dr., M/S 423
Las Vegas, Nevada 89109

A. Segrest
M&O
101 Convention Center Dr., M/S 423
Las Vegas, Nevada 89109

L. Shepherd
Sandia National Laboratories
M/S 1333
P.O. Box 5800
Albuquerque, NM 87185-1333

W. Simecka
YMSCO
P.O. Box 98518
Las Vegas, NV 89193-8518

A.Simmons
YMSCO
Department of Energy
P.O. Box 98518
Las Vegas, Nevada 89193-8518

E. Smistad
YMSCO
Department of Energy
P.O. Box 98518
Las Vegas, Nevada 89193-8518

M. Smith
YMSCO
Department of Energy
P.O. Box 98518
Las Vegas, Nevada 89193-8518

L. Snow
Roy F. Weston, Inc.
955 L'Enfant Plaza, SW
Washington, DC 20024

R. Spence
YMSCO
Department of Energy
P.O. Box 98518
Las Vegas, Nevada 89193-8518

H. Spieker
Nuclear Waste Mgmt. System
101 Convention Ctr Dr.
Las Vegas, NV 89109-2005

D. Stahl
M&O
101 Convention Ctr. Drive, M/S 423
Las Vegas, NV 89109

D. Stucker
YMSCO
Department of Energy
P.O. Box 98518
Las Vegas, Nevada 89193-8518

M. Tynan
YMSCO
Department of Energy
P.O. Box 98518
Las Vegas, Nevada 89193-8518

A. Van Luik
M&O
101 Convention Ctr. Dr., M/S 423
Las Vegas, NV 89109

G. Vawter
M&O TRW
101 Convention Center Dr.
Las Vegas, NV 89109

M. Voegele
Science Applications International Corp.
101 Convention Center Dr., #407
Las Vegas, NV 89109-2005

D. Williams
YMSCO
Department of Energy
P.O. Box 98518
Las Vegas, Nevada 89193-8518

J. Younker
M&O/TRW
101 Convention Center Dr.
Las Vegas, NV 89109

P. Zielinski
YMSCO
Department of Energy
P.O. Box 98518
Las Vegas, Nevada 89193-8518